

Get Clarity On Generics

Cost-Effective CT & MRI Contrast Agents



FRESENIUS
KABI

WATCH VIDEO

AJNR

This information is current as
of August 1, 2025.

Posterior fossa ring-enhancing lesions in the adult immunocompetent host: illustrative cases, systematic review, and proposed diagnostic algorithm

Elisabeth Van Boxtael, Alexia de Hennin, Eric Vigneul, Pasquale Scoppettuolo, Souraya El Sankari, Anna Paola Bocchio, Serena Borrelli, Valentina Lolli, Vincent van Pesch, Sofia Maldonado Sootjes, Patrice Finet, Alex Rovira, Daniel S Reich and Pietro Maggi

AJNR Am J Neuroradiol published online 29 January 2025
<http://www.ajnr.org/content/early/2025/01/29/ajnr.A8677>

SYSTEMATIC REVIEW/META-ANALYSIS

Posterior fossa ring-enhancing lesions in the adult immunocompetent host: illustrative cases, systematic review, and proposed diagnostic algorithm

Elisabeth Van Boxstael, MD,^{1*} Alexia de Hennin, MD,^{1*} Eric Vigneul, MD,^{2,3*} Pasquale Scoppettuolo, MD,¹ Souraya El Sankari, MD, PhD,¹ Anna Paola Bocchio, MD,⁴ Serena Borrelli, MD,^{5,6} Valentina Lolli, MD,⁷ Vincent van Pesch, MD, PhD,¹ Sofia Maldonado Slootjes, MD,^{8,9} Patrice Finet, MD,² Alex Rovira, MD,¹⁰ Daniel S Reich, MD, PhD,¹¹ Pietro Maggi, MD, PhD,^{1,6}

* These authors contributed equally

ABSTRACT

PURPOSE: Posterior fossa ring-enhancing lesions (PFREL) in the adult immunocompetent hosts pose a diagnostic challenge. We aimed to evaluate the spectrum of PFREL etiologies and propose a diagnostic algorithm.

METHODS: This study involved a retrospective analysis of PFREL cases from our institution (January 2023 to April 2024) and a systematic literature review conducted using Embase and PubMed databases following the PRISMA 2020 guidelines. Clinical and radiological features from these cases formed the basis of a diagnostic algorithm, which was further refined via an additional comprehensive literature review, and finally validated on an independent set of PFREL cases.

RESULTS: The systematic review (467 studies, 56 selected after inclusion/exclusion criteria) revealed that PFREL etiology was infectious in 52%, tumoral in 38% and inflammatory in 2% of cases. At initial presentation, mean age was 48 years and 36% of patients had multiple PFREL. Headache was the most common symptom (46%). Among those with reported outcomes, 36% showed complete resolution of symptoms, 29% showed improvement with residual symptoms, and 16% died. The diagnostic algorithm was created from a total of 116 PFREL cases (10 from our institutional series, 56 from the systematic literature review and 50 supplementary cases found in the literature) and included 29 possible PFREL etiologies. In the validation set (16 patients), the algorithm provided the correct diagnosis in each case.

CONCLUSION: PFREL in immunocompetent adults encompass a broad differential diagnosis. Our algorithm integrates clinical and radiologic data to assist in identifying the underlying cause of PFREL, potentially reducing the need for neurosurgical biopsy. This approach aims to enhance diagnostic accuracy, leading to better treatment decisions and improved patient outcomes.

ABBREVIATIONS: ADEM = acute disseminated encephalomyelitis; CLL = chronic lymphocytic leukemia; CSF = cerebrospinal fluid; DLBCL: diffuse large B cell lymphoma; FLAIR = fluid attenuated inversion recovery; MeSH = medical subject headings; MRI = magnetic resonance imaging; NIHSS = National Institutes of Health Stroke Scale; NMOSD = neuromyelitis optic spectrum disorder; PFREL = posterior fossa ring enhancing lesion; PRISMA = Preferred Reporting Items for Systematic reviews and Meta-Analyses; SUV max = maximum standardized uptake value.

Received September 26, 2024; accepted after revision January 18, 2025.

1. Department of Neurology, Cliniques Universitaires Saint-Luc, Université catholique de Louvain, Brussels, Belgium
2. Department of Neurosurgery, Cliniques Universitaires Saint-Luc, Université catholique de Louvain, Brussels, Belgium
3. Laboratory of Neural Differentiation (NEDI), Animal Molecular and Cellular Biology Group, Louvain Institute of Biomolecular Science and Technology, Université catholique de Louvain, Louvain-La-Neuve, Belgium
4. Department of Radiology, Cliniques Universitaires Saint-Luc, Université catholique de Louvain, Brussels, Belgium
5. Department of Neurology, Hôpital Erasme, Université Libre de Bruxelles, Brussels, Belgium
6. Neuroinflammation Imaging Lab (NIL), Institute of NeuroScience, Université catholique de Louvain, Brussels, Belgium
7. Department of Radiology, Hôpital Erasme, Hôpital Universitaire de Bruxelles, Université Libre de Bruxelles, Brussels, Belgium
8. Department of Neurology, UZ Brussel, Vrije Universiteit Brussel, Brussels, Belgium
9. NEUR Research Group, Vrije Universiteit Brussel, Brussels, Belgium
10. Section of Neuroradiology, University Hospital Vall d'Hebron, Barcelona, Spain
11. Translational Neuroradiology Section, National Institute of Neurological Disorders and Stroke, National Institutes of Health, Bethesda, MD, USA

PM research activity is supported by the Fondation Charcot Stichting Research Fund 2023 and 2025, the Fund for Scientific Research (F.R.S., FNRS; grant #40008331), Cliniques universitaires Saint-Luc "Fonds de Recherche Clinique", Biogen and Sanofi.

DSR is supported by the Intramural Research Program of the National Institute of Neurological Disorders and Stroke (NIH), USA.

On behalf of all authors, the corresponding author states that there is no conflict of interest.

Please address correspondence to Pietro Maggi, Cliniques Universitaires Saint-Luc, Av. Hippocrate 10, 1200 Brussels, Belgium. Phone number: +32 27641111; e-mail: pietro.maggi@uclouvain.be.

INTRODUCTION

Magnetic resonance imaging (MRI) of posterior fossa ring enhancing lesions (PFREL) on post-gadolinium T1-weighted images is challenging for radiologists, neurologists, and neurosurgeons.^{1,2} Indeed, a careful evaluation during the diagnostic and prognostic work-up of PFREL can guide treatment decisions and improve patient outcomes.^{3,4} The differential diagnosis of PFREL includes neoplastic, infectious, and inflammatory etiologies, with substantial variability in terms of prevalence, clinical, and radiological presentation.³⁻⁵

The diagnostic work-up should start by analyzing the clinical presentation of the patient showing PFREL: a sudden onset of symptoms is consistent with cerebrovascular events and traumatic lesions, while a subacute progression of the clinical course points toward inflammatory and neoplastic etiologies.⁶ From a radiological point of view, considering the location of the lesion within the posterior fossa is also highly informative. Indeed, differentiating between intra- and extra-axial lesions, and between midline and hemispheric PFREL of the cerebellum can aid the diagnostic work-up by excluding or suggesting some specific etiologies.⁷ In the same way, the presence of perilesional edema is a meaningful feature, as well as the pattern of enhancement, including the regularity and the completeness of the ring.³ The presence of multiple ring lesions is also a key information to guide the diagnostic approach.⁴

With this background and focusing on the adult immunocompetent host, this study aimed to: 1) show representative examples of PFREL on MRI by reporting 10 consecutive cases from our institution (including less common PFREL etiologies such as subacute ischemia and Richter syndrome), 2) describe the clinical and radiological characteristics of a wide range of PFREL diagnoses through a systematic review of the literature and, 3) propose a diagnostic algorithm for PFREL diagnosis.

MATERIALS AND METHODS

Case series

We included immunocompetent adult patients with PFREL diagnosed and treated at our institution between January 2023 and April 2024. A patient was considered immunocompetent if not suffering from any disease or underlying condition affecting immunity or taking any immunosuppressive medication (including steroids). Clinical, laboratory and MRI information, were retrospectively reviewed for each patient.

Systematic review of the literature

This systematic review was performed according to the guidelines of the Preferred Reporting Items for Systematic reviews and Meta-Analyses (PRISMA) 2020. A literature search was performed using Medical Subject Headings (MeSH) and keywords in the following databases: Embase and PubMed. The search was limited to English-language literature using the following terms: (ring enhancing lesion OR rim enhancing lesion) AND (infratentorial OR brainstem OR cerebellum OR cerebellar OR posterior fossa). Articles about PFREL published between January 1981 and November 2024 were included. Meta-analyses, reviews of the literature and congress abstracts were excluded. The data were extracted from the article text, tables, and figures. Three investigators (EVB, AdH, and EV) independently reviewed the full texts of all eligible articles. The data extracted from the articles included neurological presentation, imaging data, cerebrospinal fluid characteristics, etiology, treatment, and outcomes.

Diagnostic algorithm

Based on the PFREL cases from our institution and the literature review, we developed a diagnostic algorithm. This algorithm was designed to provide a unique and exclusive diagnosis based solely on the available clinical and radiological data, excluding any information from a potential neurosurgical biopsy (except the final diagnosis). To properly feed the algorithm, we searched for other cases in the literature matching the final diagnoses found during the systematic review, with the aim of having, as far as possible, several clinical cases per diagnosis. To do so, we conducted more in-depth searches for PFREL in PubMed and Embase, linking all diagnoses resulting from both our systematic review and case series to the MeSH used in the systematic review (e.g., associating the diagnosis “abscess” AND “infratentorial” OR “brainstem” OR “cerebellum” OR “posterior fossa”). As an additional strategy, we also used Google Reverse Image Search (also called Search by Image or Inside Search), as previously described.^{8,9} To limit confirmation biases, the algorithm was then run blindly by two authors (EVB, AdH) on a subset of randomly selected patients and adapted until achieving a perfect match between the output results and the actual diagnosis.

The algorithm was finally validated on an additional set of PFREL patients randomly selected from the literature and other institutions.

Institutional Review Board Statement

Patients sign a charter on admission to hospital stipulating that imaging and clinical information, collected for routine diagnostic procedures or patient care, may be used for retrospective academic research, without further informed consent (ethics approval 2007/10SEP/233).

RESULTS

Case series

Our consecutive case series included 10 patients (age range 18-82 years old). Clinical and radiological information are summarized in the Supplementary Table 1. Biopsy or resection was performed in 6 cases: 4 with a clear suspicion of tumoral etiology, and two (case 1 and case 2) in which the specific etiology was unclear.

Representative PFREL cases from our institutional case series are reported here below, and the corresponding MRI findings are summarized in Figure 1.

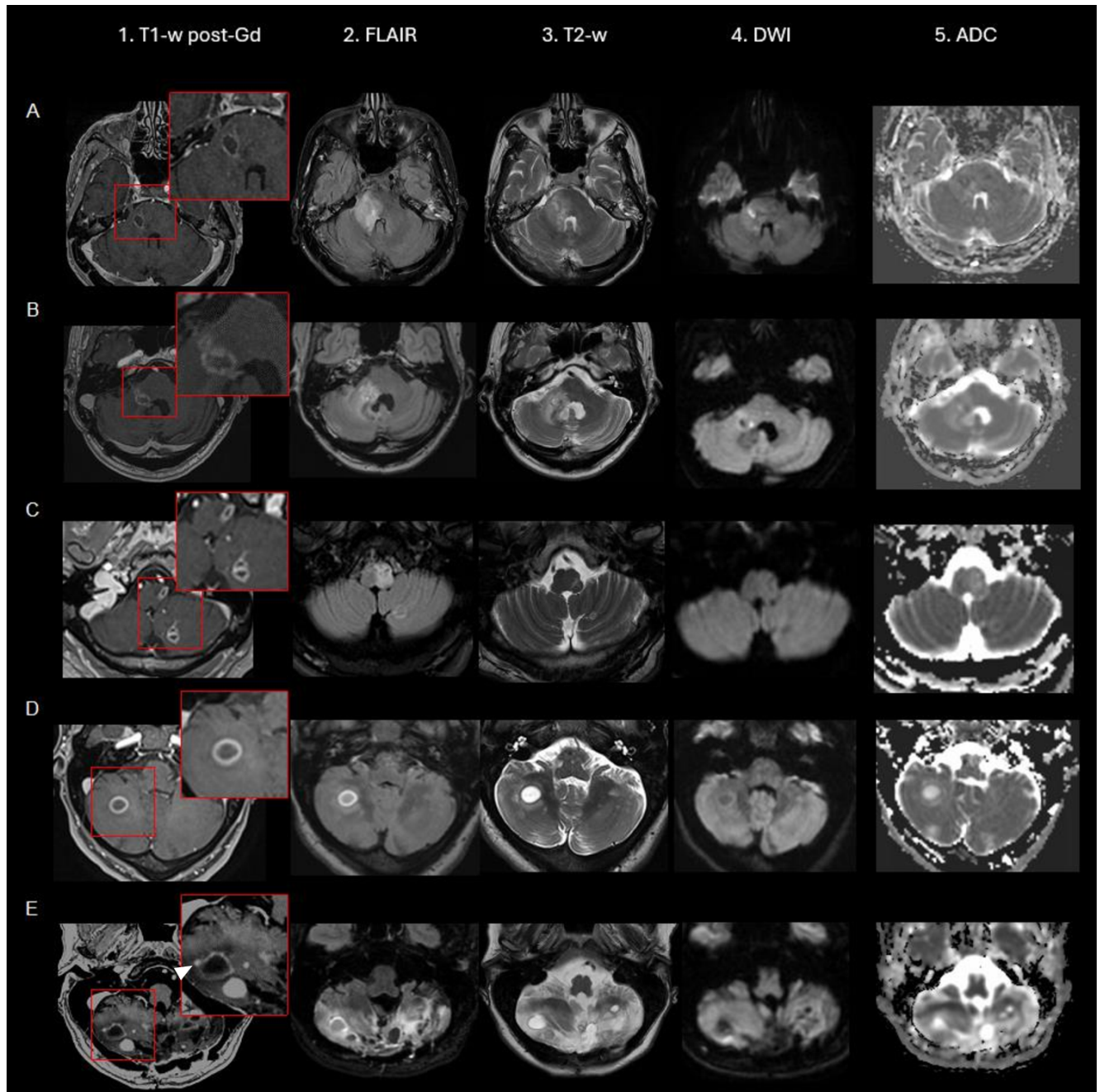


FIG 1. Brain MRI of representative PFREL cases from our institutional case series. Clinical cases corresponding to A) Richter's syndrome, B) radionecrosis, C) subacute ischemic stroke, D) multiple sclerosis, and E) hemangioblastoma (mural nodule, arrowhead). *Abbreviations:* T1-w post-Gd, T1-weighted post-gadolinium injection; FLAIR, fluid attenuated inversion recovery; T2-w, T2-weighted; DWI, diffusion weighted image; ADC, apparent diffusion coefficient.

Case 1: Richter's syndrome

A 73-year-old woman with a recent diagnosis of chronic lymphocytic leukemia (CLL) presented to another institution with progressive bilateral hearing loss and gait instability for five months. Brain MRI revealed a PFREL with a maximum diameter of 19 mm, infiltrating the right cerebellar hemisphere and the ipsilateral margin of the pons. It was surrounded by moderate vasogenic edema and caused a mild mass effect with deformation of the fourth ventricle. The lesion showed restricted diffusion in the center (Figure 1A). Lumbar puncture revealed predominantly lymphocytic pleocytosis (26 cells/mcl), with CLL-type lymphomatous lymphocytes on the examined slide. Flow cytometry revealed a low-intensity membrane Kappa monotypic B population. This CD19+ CD5+ population weakly expressed CD20. This monotypic B population presented a phenotype compatible with the CLL known to the patient, representing 31% of the encountered lymphocytes. The cerebrospinal fluid (CSF) analysis revealed hyperproteinemia (74 mg/dL) with CSF-restricted oligoclonal bands. The presence of LLC-type lymphomatous lymphocytes was confirmed on the examined slides. Infectious serologies (CMV, EBV, HIV, HBV, HCV, and syphilis) were negative. 11C-Methionine PET, to look for high grade glioma, was normal. Clinically, the patient showed deterioration, with dysarthria, multidirectional nystagmus, right hemifacial hypoesthesia, facial palsy, and abducens nerve palsy, with left hemisensory syndrome and prominent proprioceptive ataxia. The patient underwent brain biopsy, which was in favor of diffuse large B-cell lymphoma. In the context of CLL, this is suggestive of Richter's syndrome, the conversion of CLL to lymphoma, but a concomitant de novo diffuse large B cell lymphoma (DLBCL) could not be excluded. Chemotherapy with rituximab, methotrexate, procarbazine, and vincristine was initiated. Unfortunately, response to therapy was poor and palliative care was introduced.

Case 2: radionecrosis

A 54-year-old man had a history of posterior fossa ependymoma. He underwent surgery two times (two years before MRI), and resection was considered gross total. He then underwent radiotherapy (59.4 Gy in total). Two years after the end of adjuvant treatment, he developed abnormal gait. Brain MRI revealed an irregular ring-enhancing lesion in the right middle cerebellar peduncle. The lesion featured necrotic components, no restricted diffusion, and was surrounded by moderate vasogenic edema with mild mass effect. The imaging findings suggested either recurrence or radionecrosis, with radionecrosis being the more likely diagnosis due to the absence of restricted diffusion (Figure 1B). To distinguish between these two potential diagnoses, the patient underwent 11C-methionine PET. The maximum standardized uptake value (SUV max) was 2.8 at the level of the right cerebellar peduncle versus 2.0 in the left one. Subsequently, as the patient's symptoms worsened, a neurosurgical biopsy was performed, which confirmed the diagnosis of radionecrosis.

Case 3: subacute ischemic stroke

A 56-year-old man with a past medical history of diabetes, arterial hypertension, and smoking developed sudden-onset instability, right sensory loss, dysarthria, and dysphagia. The symptoms persisted but became less severe over the following days. Ten days after symptom onset, he presented to the emergency department of our institution. His National Institutes of Health Stroke Scale (NIHSS) score was 2 (dysarthria, hypoesthesia). Brain MRI revealed two focal FLAIR hyperintense lesions in the left hemi medulla oblongata and left cerebellum, as well as one confluent cortico-subcortical right parietal hyperintense lesion. Interestingly, post-gadolinium T1-weighted images showed a ring-like pattern of enhancement for the bulbar and cerebellar lesions, without associated diffusion restriction (Figure 1C). A cortico-subcortical right parietal lesion, suggestive of an old infarct was also identified (Figure 2A). A follow-up MRI 24 days after symptom onset revealed a decrease in the size of the medulla oblongata and cerebellar lesions, with some persistent enhancement on post-gadolinium T1-weighted images. The evolution of these lesions on MRI suggested an ischemic etiology. Moreover, follow-up imaging performed 3 months later (Figure 2B) revealed a FLAIR hyperintense sequela, with a highly typical pattern for a medullary infarct (anterolateral pattern with associated cerebellar involvement), without any new lesions, and an extensive work-up (autoimmune and serologic testing, lumbar puncture, PET-CT) was negative; thus, we concluded that the patient had experienced a subacute stroke involving the posteriorinferior cerebellar artery territory.

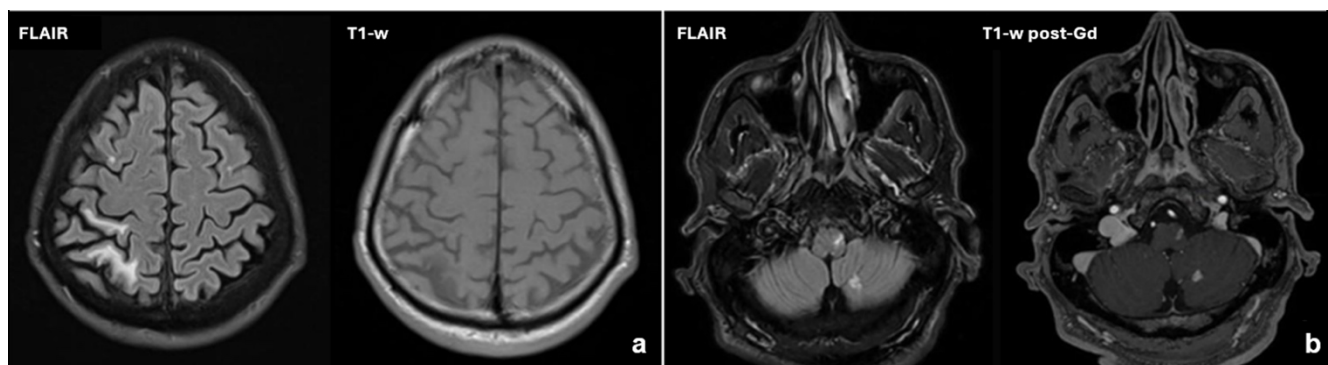


FIG 2. Imaging data of case 3 (subacute ischemic stroke). Subcortical right parietal lesion was hyperintense on FLAIR and hypointense on T1-w (a). Follow-up imaging at 4 months (b) revealed a FLAIR hyperintense sequela with nodular enhancement on T1-w post-Gd images, with a highly typical pattern for a medullary infarct (anterolateral pattern with associated cerebellar involvement). *Abbreviations:* FLAIR, fluid attenuated inversion recovery; T1-w, T1-weighted images; T1-w post-Gd, T1-weighted post-gadolinium injection.

Case 4: multiple sclerosis

An 18-year-old woman presented with subacute onset of gait disorder. Brain MRI revealed a PFREL with mild surrounding edema, no diffusion restriction in the lesion center and a thin rim of peripheral restricted diffusion (Figure 1D). Moreover, brain MRI showed multiple infratentorial and supratentorial white-matter lesions, some of them showing contrast enhancement on T1-w post-Gd images, suggesting an inflammatory demyelinating etiology (Figure 3a). Lumbar puncture revealed typical CSF-restricted oligoclonal bands, and the patient was treated with methylprednisolone. Finally, thanks to the presence of a dissemination in time on brain MRI, a final diagnosis of multiple sclerosis was established. A follow-up MRI performed 2 months after the initial appearance of the cerebellar inflammatory lesion showed disappearance of the T1-w post-Gd enhancing ring, without recurrence of any lesional acute inflammatory activity on the 6 years follow-up MRI (Figure 3c).

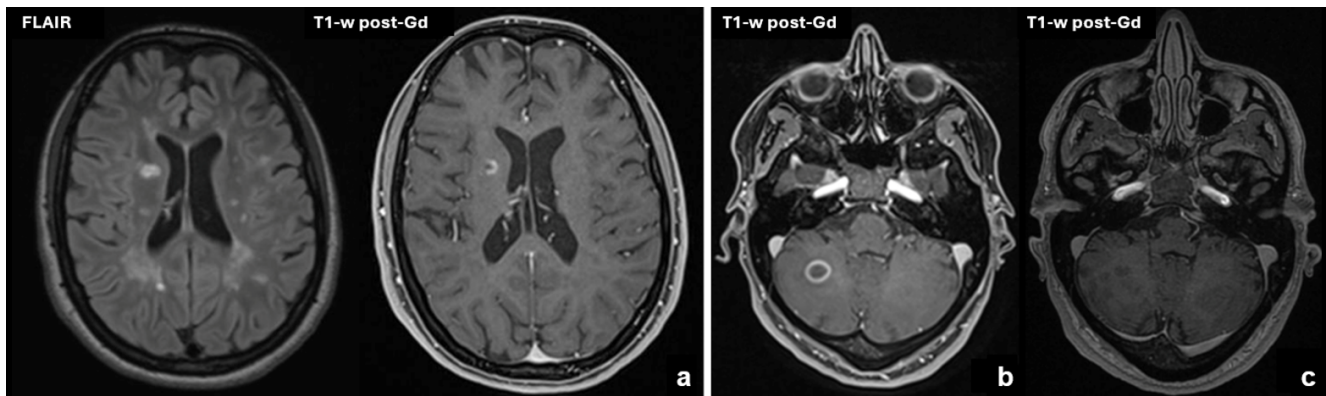


FIG 3. Imaging data of case 4 (multiple sclerosis). Multiple supratentorial lesions (a) were identified on FLAIR, one of them with incomplete enhancing ring (horseshoe-like) on T1-w post-Gd images. Follow-up MRI show a complete disappearance of the enhancement (c) 2 months after the initial ring enhancing pattern (b). *Abbreviations:* FLAIR, fluid attenuated inversion recovery; T1-w post-Gd, T1-weighted post-gadolinium injection.

Case 5: hemangioblastoma

A 43-year-old woman was followed at our institution for Von Hippel-Lindau disease, diagnosed at age 14 (p.Asp-78Ser mutation in exon 1). She has undergone several surgeries for posterior fossa hemangioblastomas. Her brain MRI showed multiple infratentorial nodular and cystic lesions, one featuring a clear peripheral contrast enhancement compatible with PFREL. This PFREL was associated with a typical mural nodule (Figure 1E).¹⁰

Systematic review of the literature

Our electronic search yielded 467 studies. After applying the inclusion criteria, exclusion criteria, and full-text examination, 56 articles were included in the analysis. A PRISMA flow diagram specifying the data collected and evaluated is provided in Figure 4. The data corresponding to this literature review are summarized in Supplementary Table 2 (clinical characteristics, treatment, outcome, MRI details and ancillary exams) and Supplementary Table 3 (patients' characteristics).

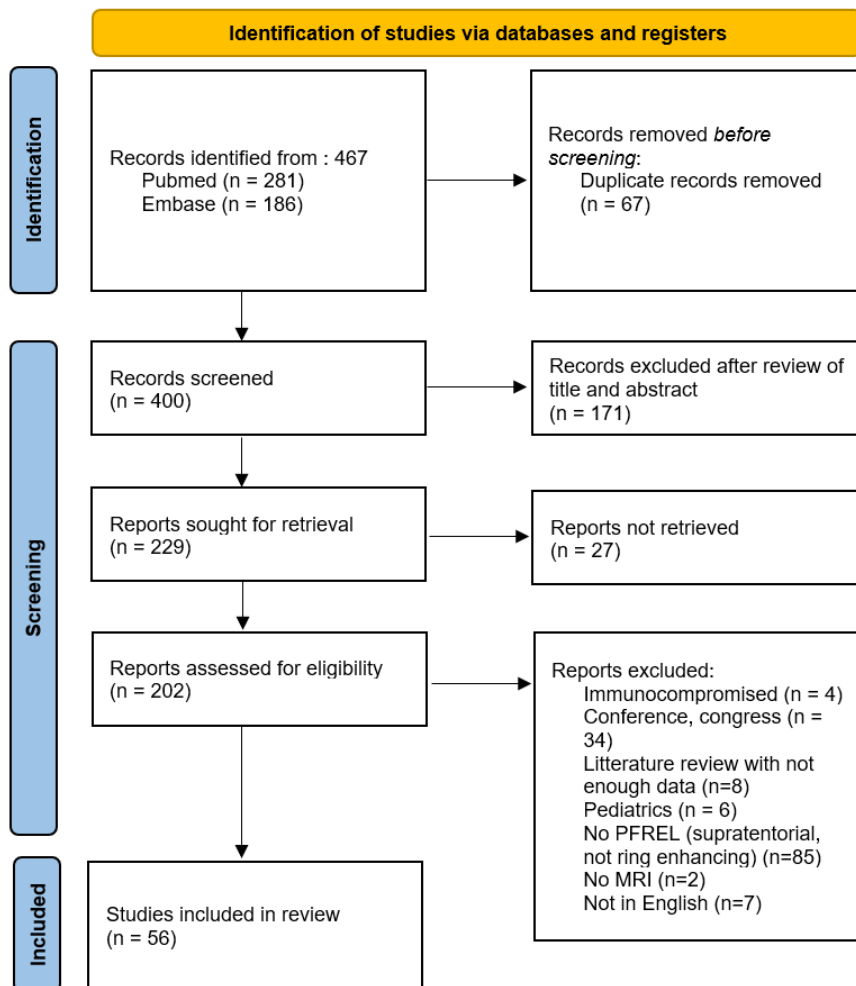


FIG 4. PRISMA 2020 flowchart

Of the 56 included patients with PFREL, 16 were female (29%). The mean age was 47.9 years old (± 18.5 SD; median 47; range 18-82 years). Fourteen originated from North America, 4 from Africa, 3 from South America, 5 from Europe, 1 from Australia and 29 from Asia.

Headache was the most common symptom (46%), followed by instability (34%), visual disturbances (29%), hemiparesis (23%), and nausea (20%). Symptoms had been present for one month or more prior to diagnosis in 19 patients (34%).

The specific etiology was infectious in 52% of the patients (29/56), tumoral in 38% (21/56) and inflammatory in 2% (6/56). More than one PFREL was found in 36% (20/56) of the patients. Among these 20 patients, PFREL etiology was infectious in 11, tumoral in 6, and inflammatory in 3. Among those for whom information was available (17/42), the median PFREL size was 2.35 cm (range 0.9-4.8) in patients with a tumoral etiology and 2.25 cm (range 0.9-2.9) in those with infections. This data was not available with PFREL of inflammatory etiology.

Chest imaging was not reported or was reported as normal in 39 (70%) patients. In the 13 patients with abnormalities (30%), interstitial pneumonia, prominent pulmonary arteries, atelectasis, pulmonary nodules, granulomas, masses, opacities, lymphadenopathies, and/or miliary tuberculosis were reported. Twenty-three patients (41%) had CSF analysis, among which 18 (32%) had abnormalities (pleocytosis, high level of CSF proteins, and/or presence of oligoclonal bands). Thirty-four patients (61%) underwent biopsy, aspiration, or resection. Among infectious etiologies, 3 patients were treated without either CSF analysis or biopsy support.

Clinical outcomes were not reported for eleven patients. Thirty-six percent (20/56) showed complete resolution of symptoms, 29% (16/56) showed improvement but had residual symptoms, and 16% (9/56) died despite treatment.

Diagnostic algorithm

Based on a total of 116 cases (10 from our institutional series, 56 from the systematic review and 50 supplementary cases found in the literature – Supplementary Table 4), we found twenty-nine possible PFREL etiologies (Supplementary Table 5). Accordingly, we designed a PFREL diagnostic algorithm combining both clinical and radiological data. The algorithm was then run blindly on a subset of patients and adapted until achieving a perfect match between the output results and the actual diagnosis. Finally, the diagnostic algorithm was validated on an independent set of 16 patients with various PFREL etiologies (Supplementary Table 6) and provided the correct diagnosis in each case.

The proposed diagnostic algorithm is reported in Figure 5 and is available online at <https://forms.office.com/e/TTjwjtFL8>.

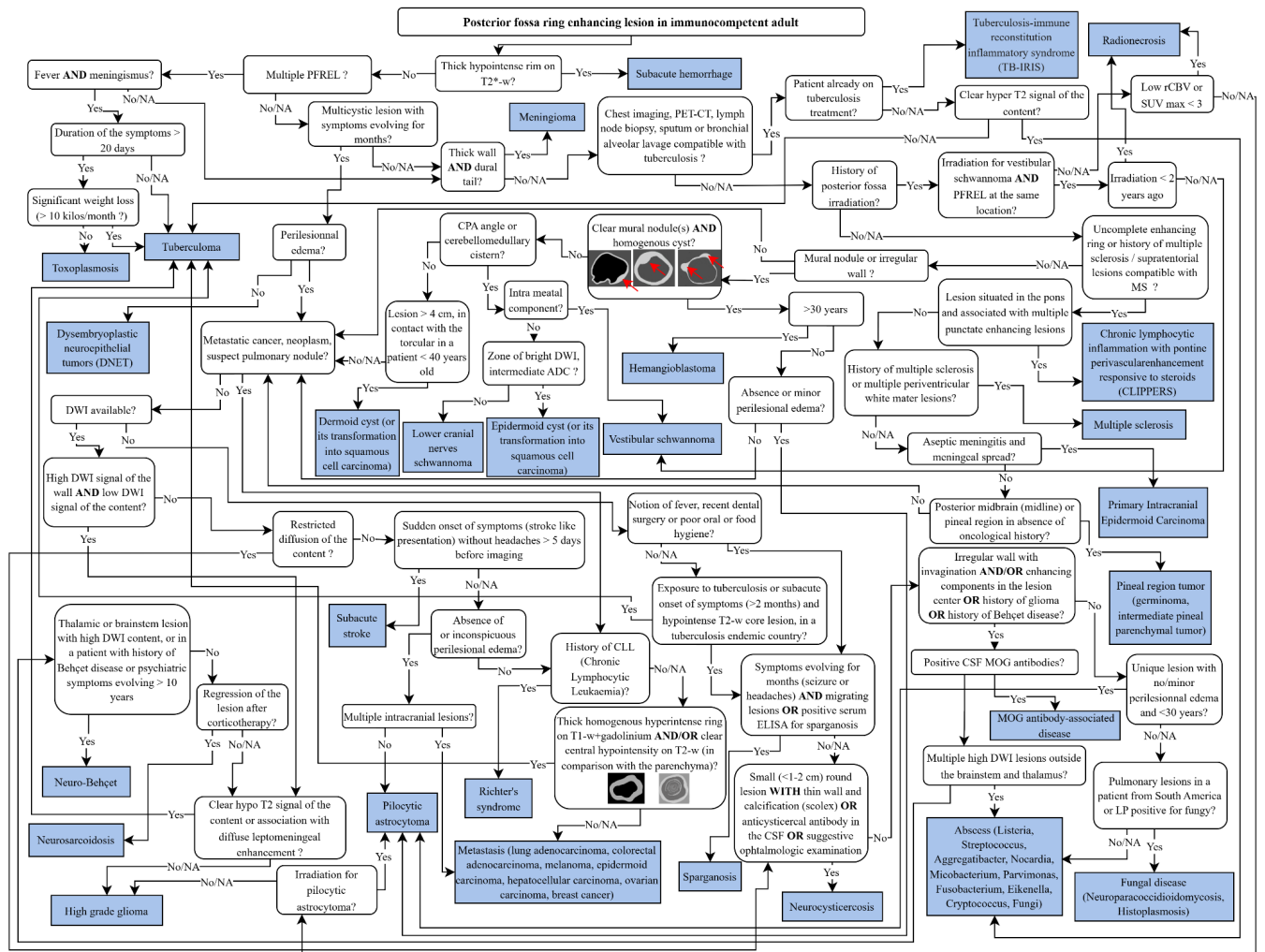


FIG 5. Diagnostic algorithm. Abbreviations: CPA cerebellopontine angle, CSF cerebrospinal fluid, DWI diffusion weighted image, LP Lumbar Puncture, MOG Myelin Oligodendrocyte Glycoprotein, PFREL posterior fossa ring-enhancing lesion, rCBV regional Cerebral Blood Volume, SUV standardized uptake value

DISCUSSION

The differential diagnosis of PFREL include at least 29 distinct conditions, mainly comprising infectious (abscess and tuberculomas) and oncologic etiologies.¹¹⁻¹³

Beyond providing a comprehensive review of PFREL etiologies, we have also developed a globally applicable PFREL diagnostic algorithm, based on clinical and radiological information to guide diagnosis and treatment decisions. The proposed algorithm highlights simple yet valuable elements (chest X-ray, dermatological examination, psychiatric history, lumbar puncture) that clinicians should consider during the diagnostic work-up. These elements emerged as key differentiating tools between different etiologies during the algorithm's development. We tried to keep our diagnostic tree as readable and practical as possible by providing an electronic version which we found easier and more intuitive to use <https://forms.office.com/e/TTjjwtjFL8>. Indeed, simplification is arduous during PFREL diagnostic work-up, as radiological presentations often lack specificity. One example is the homogeneously intralesional restricted diffusion pattern, which is not specific for abscess and can sometimes be observed also for mucoid metastases.¹⁴⁻¹⁶ Similarly, the incomplete ring enhancing pattern often observed in inflammatory demyelinating lesions, is not pathognomonic, as it has also been described in primary CNS lymphoma.¹⁷

Another challenge is to classify PFREL whose morphological aspects evolve over time, such as tuberculomas (Table 1).¹⁸⁻²⁰ Moreover in tuberculous pathologies, the radiological appearance of liquefied tuberculomas can be identical to that of tuberculous abscesses.^{19,20} Thus, in one of our 18 cases of tuberculomas, the algorithm provides the diagnosis of abscess.²¹

This systematic research and the resulting algorithm have some limitations. Indeed, these reviews, mostly based on case reports, suffer from inherent biases such as publication and selection biases. Despite their didactic format providing detailed clinico-radiological reports of individual patients, case reports favor the description of unique and original cases, often leading to an overestimation of rarer and unusual clinical and radiological presentations. Common pathologies such as metastases are probably underreported due to the lack of interest in documenting classic cases featuring more typical clinico-radiological presentations. Moreover, brain metastases are sometimes referred as "cystic" or "necrotic" rather than ring-enhancing lesions.

Additionally, some PFREL diagnoses are supported by limited data, such as the single case of primary infratentorial CNS lymphoma that we found, which was published in an imaging series and lacked sufficient clinical information to be properly included in the algorithm.²²

Finally, even if not found in our review, certain pathologies leading to lesions with supratentorial enhancing rings in immunocompetent hosts can also theoretically present in the infratentorial region, such as acute disseminated encephalomyelitis (ADEM), neuromyelitis optica spectrum disorder (NMOSD), and leukoencephalopathies.^{12,23} We acknowledge that the available literature and our current case series may not exhaust all the diagnostic possibilities for PFREL, and as such our algorithm should be applied with caution pending further validation.

Regarding the design of the algorithm, it was delicate to precisely describe the radiological characteristics intrinsic to a pathology while encompassing interindividual variabilities, leading to terms associated with a certain degree of interpretation, such as "irregular wall" or "thick wall." Adding illustrations rather than numerical data proved to be an efficient method of reducing this type of interpretation ambiguity.

CONCLUSIONS

PFREL in the adult immunocompetent host encompasses a broad differential diagnosis. By reviewing representative cases from our institution and performing a systematic literature search, we developed a diagnostic algorithm to guide clinicians during PFREL clinical work-up. We also described two etiologies of PFREL that are rarely encountered in clinical practice: Richter's syndrome and subacute stroke. Based on our work, we conclude that the main radiological parameters guiding the diagnosis of PFREL in the immunocompetent adult are the presence or absence of other ring-enhancing lesions, presence of perilesional edema, thickness and completeness of the enhancing ring, and size and location of the lesion. The main clinical data to consider are the age of the patient, duration of symptoms, presence of infectious signs, history of neoplasm or irradiation, and contact with patients with tuberculosis, or origin from/travel in areas endemic for this disease. Important complementary examinations to perform are chest imaging and, if not contraindicated, lumbar puncture. This proposed systematic approach aims to enhance diagnostic accuracy, support better treatment decisions, and improve patient outcomes, as well as potentially reduce the need for neurosurgical biopsy.

Table 1: Radiographic features of intracranial tuberculosis

	Non-caseating granuloma	Caseating granuloma	Caseating granuloma with central liquefaction	Calcified granuloma	Tuberculous abscess
T1-w	Iso- to hypointense	Iso- to hypointense with hyperintense rim	Iso- to hypointense with hyperintense rim	Iso- to hypointense	Central low intensity (hyperintense to CSF)
T1-w post-Gd	Homogenous enhancement	Homogeneous or ring-enhancement	Ring enhancement	No enhancement	Ring enhancement
T2-w	Hyperintense	Hypointense Surrounded by vasogenic edema	Hypointense rim with central hyperintensity Surrounded by vasogenic edema	Hypointense	Central high intensity Abscess capsule may be visible as an intermediate to slightly low signal thin rim Surrounded by vasogenic edema
DWI	No restricted diffusion	No restricted diffusion	Variable diffusion restriction	No restricted diffusion	High DWI signal is usually present centrally

Abbreviations: CSF, cerebrospinal fluid; T1-w, T1-weighted; T1-w post-Gd, T1-weighted post gadolinium; T2-w, T2-weighted, DWI, diffusion weighted image

REFERENCES

- Li L, Xie HM, Richard SA, Lan Z. Hemangioblastoma masquerading as a ring enhancing lesion in the cerebellum A case report. *Med U S*. 2022;101(3):E28665.
- Goto Y, Ebisu T, Mineura K. Abscess formation within a cerebellar metastasis: Case report and literature review. *Int J Surg Case Rep*. 2015;10:59–64.
- Filippi M, Preziosa P, Banwell BL, Barkhof F, Ciccarelli O, De Stefano N, et al. Assessment of lesions on magnetic resonance imaging in multiple sclerosis: practical guidelines. *Brain*. 2019 Jul 1;142(7):1858–75.
- Smirniotopoulos JG, Jäger HR. Differential Diagnosis of Intracranial Masses. In: Hodler J, Kubik-Huch RA, von Schulthess GK, editors. *Diseases of the Brain, Head and Neck, Spine 2020–2023: Diagnostic Imaging* [Internet]. Cham (CH): Springer; 2020 [cited 2024 Jun 20]. (IDKD Springer Series). Available from: <http://www.ncbi.nlm.nih.gov/books/NBK554352/>
- Gaillard F. Radiopaedia. [cited 2024 Jun 20]. Ischemic stroke | Radiology Reference Article | Radiopaedia.org. Available from: <https://radiopaedia.org/articles/ischaemic-stroke>
- Wildner P, Stasiulek M, Matysiak M. Differential diagnosis of multiple sclerosis and other inflammatory CNS diseases. *Mult Scler Relat Disord*. 2020 Jan 1;37:101452.
- Nair S, Baldawa SS, Gopalakrishnan CV, Menon G, Vikas V, Sudhir JB. Surgical outcome in cystic vestibular schwannomas. *Asian J Neurosurg*. 2016 Sep;11(3):219.
- Mamrosh JL, Moore DD. Using Google Reverse Image Search to Decipher Biological Images. *Curr Protoc Mol Biol*. 2015 Jul 1;111:19.13.1-19.13.4.
- Sharifzadeh A, Das S, Smith GP. Google reverse image search using dermatology eConsult cases. *Dermatol Ther*. 2020 Nov;33(6):e14372.
- Kim EH, Moon JH, Kang SG, Lee KS, Chang JH. Diagnostic challenges of posterior fossa hemangioblastomas: Refining current radiological classification scheme. *Sci Rep*. 2020 Apr 14;10:6267.
- Garg RK, Desai P, Kar M, Kar AM. Multiple ring enhancing brain lesions on computed tomography: An Indian perspective. *J Neurol Sci*. 2008 Mar 15;266(1):92–6.
- Garg RK, Paliwal V, Pandey S, Uniyal R, Agrawal KK. The etiological spectrum of multiple ring-enhancing lesions of the brain: a systematic review of published cases and case series. *Neurol Sci Off J Ital Neurol Soc Ital Soc Clin Neurophysiol*. 2024 Feb;45(2):515–23.
- Patel A, More B, Rege I, Ranade D. Clinical diagnosis and management of multiple cerebral ring-enhancing lesions-study of 50 patients at a tertiary healthcare center. *J Cancer Res Ther*. 2024 Jan 1;20(1):112–7.
- Yasuda C, Okada K, Takechi U, Tsuji S. Ring-enhanced brainstem lesion in a patient with neuro-Behçet's disease. *Intern Med Tokyo Jpn*. 2012;51(8):991–2.
- Garg RK, Sinha MK. Multiple ring-enhancing lesions of the brain. *J Postgrad Med*. 2010 Dec;56(4):307.
- Feraco P, Donner D, Gagliardo C, Leonardi I, Piccinini S, Del Poggio A, et al. Cerebral abscesses imaging: A practical approach. *J Popul Ther Clin Pharmacol J Ther Popul Pharmacol Clin*. 2020 Jul 11;27(3):e11–24.
- Zhang D, Hu LB, Henning TD, Ravarani EM, Zou LG, Feng XY, et al. MRI findings of primary CNS lymphoma in 26 immunocompetent patients. *Korean J Radiol*. 2010;11(3):269–77.
- Sadashiva N, Tiwari S, Shukla D, Bhat D, Saini J, Somanna S, et al. Isolated brainstem tuberculomas. *Acta Neurochir (Wien)*. 2017 May;159(5):889–97.
- Mahomed N, Kilborn T, Smit EJ, Chu WCW, Young CYM, Koranteng N, et al. Tuberculosis revisited: classic imaging findings in childhood. *Pediatr Radiol*. 2023 Aug;53(9):1799–828.
- Intracranial tuberculous granuloma | Radiology Reference Article | Radiopaedia.org [Internet]. [cited 2024 Nov 16]. Available from: <https://radiopaedia.org/articles/intracranial-tuberculous-granuloma>
- Chan K, Siu J. Magnetic Resonance Imaging Features of Cerebral Ring-Enhancing Lesions with Different Aetiologies. *Hong Kong J Radiol*. 2021 Mar 25;24(1):62–74.
- Sutherland T, Yap K, Liew E, Tartaglia C, Pang M, Trost N. Primary central nervous system lymphoma in immunocompetent patients: a retrospective review of MRI features. *J Med Imaging Radiat Oncol*. 2012 Jun;56(3):295–301.
- Lim KE, Hsu YY, Hsu WC, Chan CY. Multiple complete ring-shaped enhanced MRI lesions in acute disseminated encephalomyelitis. *Clin Imaging*. 2003;27(4):281–4.
- Adachi J, Uki J, Kazumoto K, Takeda F. Diagnosis of brainstem abscess in the cerebritis stage by magnetic resonance imaging--case report. *Neurol Med Chir (Tokyo)*. 1995 Jul;35(7):467–70.
- Alhamshari YSM, Punjabi C, Pressman GS, Govil A. Sinus venous atrial septal defect presenting with brain abscesses in a 77-year-old immunocompetent patient. *BMJ Case Rep*. 2015 Oct 16;2015:bcr2015212165.
- Alharbi A, Khairy S, Al Sufiani F, Alkhani A. Intracranial tuberculomas: A case report of clinical, radiological, and pathological characteristics. *Int J Surg Case Rep*. 2021 Nov;88:106477.
- Arif S, Arif S, Slehria AUR, Yousaf G, Nawaz KH. Central Nervous System Tuberculosis With Shower Like Pattern of Intracranial Tuberculomas in an Immunocompetent Patient. *Cureus*. 2020 Aug 21;12(8):e9922.
- Besada CH, Migliaro M, Christiansen SB, Funes JA, Ajler PM, Mónaco RDG. Restricted diffusion in a ring-enhancing mucoid metastasis with histological confirmation: Case report. *J Comput Assist Tomogr*. 2010;34(5):770–2.
- Bhattacharjee S, Majumdar A, Jana A. Headache and central positioning vertigo in a middle aged female-a case of solitary cerebellar tuberculoma involving left cerebellar hemisphere. *Turk Noroloji Derg*. 2012;18(1):39–42.
- Capone S, Emechebe D, St Clair EG, Sadr A, Feinberg M. Presentation, diagnosis, and treatment of a cerebellar tuberculoma: illustrative case. *J Neurosurg Case Lessons*. 2021 Nov 1;2(18):CASE21170.
- Chin HH, Yap YL, Chin YH, Lim HH, Chang A, Chua HH. Case Report: Central Nervous System Tuberculosis Immune Reconstitution Inflammatory Syndrome in a Non-HIV Patient. *SN Compr Clin Med*. 2020;2(6):802–6.
- de Almeida SM, Imano ECM, Vicente VA, Gomes RR, Trentin AP, Zamarchi K, et al. Primary Central Nervous System Infection by Histoplasma in an Immunocompetent Adult. *Mycopathologia*. 2020 Apr;185(2):331–8.
- De Keersmaecker S, Van Cauter S, Bekelaar K. Multiple Ring-Enhancing Brain Lesions: Fulminant Diffuse Cerebral Toxoplasmosis or Cerebral Metastases? *Top Magn Reson Imaging*. 2024;33(2):e0311.
- Feizi P, Tandon M, Khan E, Subedi R, Prasad A, Chowdhary A, et al. Overcoming the elusiveness of neurosarcoidosis: Learning from five complex cases. *Neurol Int*. 2021;13(2):130–42.
- Fereydonyan N, Taheri M, Kazemi F. Cerebellar Squamous Cell Carcinoma Due to Malignant Transformation of Cerebellopontine Angle Epidermoid Cyst, Report an Interesting Case and Review the Literature. *Prague Med Rep*. 2019;120(2–3):95–102.
- Gottlieb M, Kogan A, Kimball D. Intracranial tuberculoma presenting as an isolated oculomotor nerve paresis. *J Emerg Med*. 2015;48(1):e1–4.
- Heo JH, Lee ST, Chu K, Kim M. Neuro-Behçet's disease mimicking multiple brain tumors: Diffusion-weighted MR study and literature review. *J Neurol Sci*. 2008;264(1–2):177–81.
- Imoto H, Nishizaki T, Nogami K, Sakamoto K, Nomura S, Akimura T, et al. Neuro-Behçet's disease manifesting as a neoplasm-like lesion--case report. *Neurol Med Chir (Tokyo)*. 2002 Sep;42(9):406–9.
- Jongeling AC, Pisapia D. Pearls and oysters: tuberculous meningitis: not a diagnosis of exclusion. *Neurology*. 2013 Jan 22;80(4):e36–39.
- Jorge LA, Yamashita S, Trindade AP, Lima Resende LA, Zanini MA, Caldeira Xavier JC, et al. Pseudotumoral neuroparacoccidioidomycosis of the posterior fossa: A case report and review of the literature. *Surg Neurol Int*. 2017;8:76.
- Kim MS, Kim OL. Primary intracranial squamous cell carcinoma in the brain stem with a cerebellopontine angle epidermoid cyst. *J Korean Neurosurg Soc*. 2008 Dec;44(6):401–4.
- Kong A, Koukourou A, Boyd M, Crowe G. Metastatic adenocarcinoma mimicking 'target sign' of cerebral tuberculosis. *J Clin Neurosci Off J*

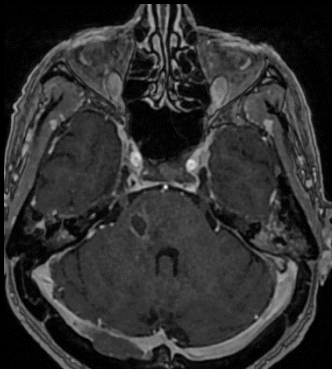
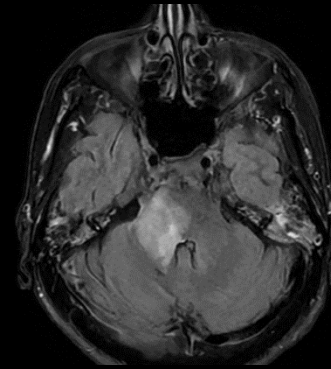

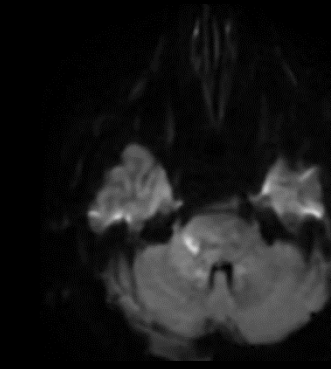
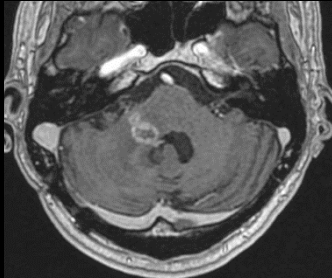
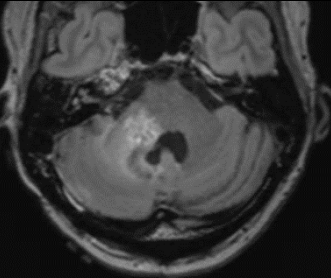
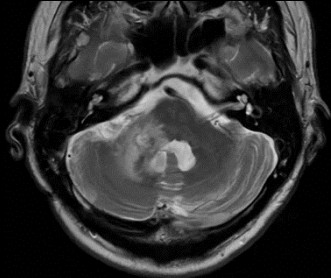
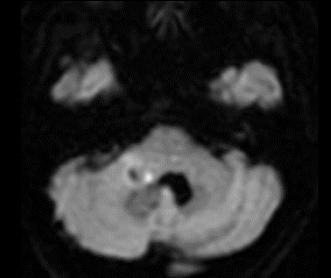
- Neurosurg Soc Australas. 2006 Nov;13(9):955–8.
43. Lakra R, Bouchette P, Rana M, Kulkarni S. Rectum to Medulla Oblongata: Colorectal Cancer Metastasizing to the Brainstem. *Cureus*. 2023 May;15(5):e39738.
44. Lath R, Rajshekhar V. Solitary cysticercus granuloma of the brainstem. *J Neurosurg*. 1998;89(6):1047–51.
45. Lee WY, Ling M, Anderson G, Achawal S, Thaker HK. Isoniazid-resistant intracranial tuberculoma treated with a combination of moxifloxacin and first-line anti-tuberculosis medication. *J Med Microbiol*. 2011;60(10):1550–2.
46. Li YX, Ramsahye H, Yin B, Zhang J, Geng DY, Zee CS. Migration: a notable feature of cerebral sparganosis on follow-up MR imaging. *AJNR Am J Neuroradiol*. 2013 Feb;34(2):327–33.
47. Lyons JL, Neagu MR, Norton IH, Klein JP. Diffusion tensor imaging in brainstem tuberculoma. *J Clin Neurosci*. 2013;20(11):1598–9.
48. Mandapat AL, Eddleman CS, Bissonnette ML, Batjer HH, Zembower TR. Idiopathic pontine *Streptococcus salivarius* abscess in an immunocompetent patient: Management lessons through case illustration and literature review. *Scand J Infect Dis*. 2011;43(11–12):837–47.
49. Maruya J, Narita E, Nishimaki K, Heianna J, Miyauchi T, Minakawa T. Primary cystic germinoma originating from the midbrain. *J Clin Neurosci Off J Neurosurg Soc Australas*. 2009 Jun;16(6):832–4.
50. Matsumoto J, Kochi M, Morioka M, Nakamura H, Makino K, Hamada JJ, et al. A long-term ventricular drainage for patients with germ cell tumors or medulloblastoma. *Surg Neurol*. 2006 Jan;65(1):74–80; discussion 80.
51. Medina-Flores R, Germanwala A, Molina JT, Meltzer CC, Wiley CA. October 2003: A 59-year-old woman with sudden onset of diplopia. *Brain Pathol*. 2004;14(2):225–6.
52. Naphade PU, Singh MK, Garg RK, Rai D. Bilateral ptosis: An atypical presentation of neurocysticercosis. *BMJ Case Rep [Internet]*. 2012;((Naphade P.U.; Singh M.K., maneesh_singh@rediffmail.com; Garg R.K.; Rai D.) Department of Neurology, Chhatrapati Shahuji Maharaj Medical University, Uttar Pradesh, Lucknow, India). Available from: <https://www.embase.com/search/results?subaction=viewrecord&id=L365527799&from=export>
53. Niu T, Tucker AM, Nagasawa DT, Bergsneider M. Solitary *Aggregatibacter aphrophilus* tectal abscess in an immunocompetent patient. *Surg Neurol Int*. 2017;8:257.
54. O'Callaghan M, Mok T, Lefter S, Harrington H. Clues to diagnosing culture negative *Listeria rhombencephalitis*. *BMJ Case Rep*. 2012 Sep 30;2012:bcr2012006797.
55. Otero-Fernández P, Ruiz-Escribano-Menchén L, Herrera-Montoro V, Morcillo-Carratalá R, Calvo-García M, Llumiguano-Zaruma C. Accessory nerve ancient schwannoma: A case report. *Surg Neurol Int [Internet]*. 2022;13((Otero-Fernández P., paulaofe@hotmail.com; Llumiguano-Zaruma C., carlos.llumiguano@yahoo.com) Department of Neurosurgery, Hospital General Universitario de Ciudad Real, Ciudad Real, Spain). Available from: <https://www.embase.com/search/results?subaction=viewrecord&id=L2019810831&from=export>
56. Parekh R, Hafika A, Porter A. A rare case of central nervous system tuberculosis. *Case Rep Infect Dis*. 2014;2014:186030.
57. Pekova L, Parusheva P, Mitev M, Dochev I, Naydenov C. A rare case of an HIV-seronegative patient with *Toxoplasma gondii* meningoencephalitis. *IDCases*. 2021;26:e01271.
58. Raheja A, Eli IM, Bowers CA, Palmer CA, Couldwell WT. Primary Intracranial Epidermoid Carcinoma with Diffuse Leptomeningeal Carcinomatosis: Report of Two Cases. *World Neurosurg*. 2016;88((Raheja A.; Eli I.M.; Bowers C.A.; Couldwell W.T., neuropub@hsc.utah.edu) Department of Neurological Surgery, University of Utah, Salt Lake City, UT, United States):692.e9–692.e16.
59. Raval V, Khetan V. Spectral domain optical coherence tomography features of subretinal cysticercus cyst. *J Ophthalmic Vis Res*. 2012 Oct;7(4):347–9.
60. Sankar J, Majumdar SS, Unniyal M, Singh H, Khullar A, Kumar K. Bilateral ptosis: An unusual presentation of mid brain tuberculoma. *Med J Armed Forces India*. 2021;77(1):96–100.
61. Shaikh MY, Sharif S, Rafay M. Primary Intracranial Squamous Cell Carcinoma Arising in Dermoid Cyst. *Asian J Neurosurg*. 2019;14(3):904–6.
62. Shih WJ, Kadzielawa K, Lee C, Moody EB, Ryo UY. Tc-99m sestamibi uptake by cerebellar metastasis from bronchogenic carcinoma. *Clin Nucl Med*. 1993 Oct;18(10):887–90.
63. Shrestha P, Sandhu MRS, Jensen KJ, Shidoh S, Yamaguchi S. Cranial nerves bridging the middle ear and cerebellum causing cerebellar peduncle abscess: A case report. *Acta Radiol Open*. 2024 Oct;13(10):20584601241279336.
64. Sinha MK, Garg RK, Anuradha HK, Agarwal A, Parihar A, Mandhani PA. Paradoxical vision loss associated with optochiasmatic tuberculoma in tuberculous meningitis: A report of 8 patients. *J Infect*. 2010 Jun;60(6):458–66.
65. Song TJ, Suh SH, Cho H, Lee KY. Claude's syndrome associated with neurocysticercosis. *Yonsei Med J*. 2010 Nov;51(6):978–9.
66. Suzuki T, Okamoto K, Genkai N, Kakita A, Abe H. A homogeneously enhancing mass evolving into multiple hemorrhagic and necrotic lesions in amoebic encephalitis with necrotizing vasculitis. *Clin Imaging*. 2020;60(1):48–52.
67. Tailor JK, Kim AH, Folkert RD, Black PM. The development of ring-shaped contrast enhancement in a case of cerebellar dysembryoplastic neuroepithelial tumor: case report. *Neurosurgery*. 2008 Sep;63(3):E609–610; discussion E610.
68. Tanaka H, Kiko K, Watanabe Y, Yaguchi T, Oya S, Shiojiri T. Miliary cerebrospinal lesions caused by *Nocardia beijingensis* in an immunocompetent patient. *IDCases [Internet]*. 2020;20((Tanaka H., hajime.tanaka.gim@gmail.com; Shiojiri T.) Department of General Internal Medicine, Asahi General Hospital, Asahi, Chiba, Japan). Available from: <https://www.embase.com/search/results?subaction=viewrecord&id=L2005114124&from=export>
69. Toshikuni N, Morii K, Yamamoto M. Radiotherapy for multiple brain metastases from hepatocellular carcinomas. *World J Gastroenterol*. 2007 Sep 7;13(33):4520–2.
70. Tsutsumi S, Horinaka N, Mori K, Maeda M. Metastatic brainstem tumor manifesting as hearing disturbance--case report. *Neurol Med Chir (Tokyo)*. 2001 Nov;41(11):561–4.
71. Uchino M, Haga D, Mito T, Kuramitsu T, Nakamura N. Primary midbrain cystic germinoma mimicking glioma: A case with neuroendoscopic biopsy. *J Neurooncol*. 2006;79(3):255–8.
72. Ueno H, Tomimura H, Yoshimoto T, Ochi K, Nomura E, Maruyama H, et al. Paroxysmal dysarthria and ataxia in chronic lymphocytic inflammation with pontine perivascular enhancement responsive to steroids. *Neurol Clin Neurosci*. 2014;2(1):13–5.
73. Utsuki S, Oka H, Kijima C, Yasui Y, Fujii K, Kawano N. Pilocytic astrocytoma with abundant oligodendroglioma-like component. *Brain Tumor Pathol*. 2012;29(2):103–6.
74. Wang L, Xie Y, Liu Y, Tan J, Chen Z, Xiao Y, et al. Brachium Pontis Gliosarcoma With Well-Differentiated Cartilaginous Tissue: A Case Report. *Medicine (Baltimore)*. 2015 Oct;94(42):e1735.
75. Yiu G, Lessell S. Dorsal midbrain syndrome from a ring-enhancing lesion. *Semin Ophthalmol*. 2012;27(3–4):65–8.
76. Almeida CC, Uzuner A, Alterman RL. Stereotactic Drainage of Brainstem Abscess With the BrainLab Varioguide™ System and the Airo™ Intraoperative CT Scanner: Technical Case Report. *Oper Neurosurg*. 2018 Apr;14(4):E46–50.
77. Byrne J, Oh KS, Wang N. Special Topics in Brain Metastases Management. In: Yamada Y, Chang E, Fiveash JB, Knisely J, editors. *Radiotherapy in Managing Brain Metastases: A Case-Based Approach [Internet]*. Cham: Springer International Publishing; 2020 [cited 2024 Jun 26]. p. 197–215. Available from: https://doi.org/10.1007/978-3-030-43740-4_14
78. Chowdhury S, Uddin N. A Case of Neurocysticercosis Clinically Mimicking Epilepsy: Report from Remote Hilly Area of Bangladesh. *Bangladesh J Infect Dis*. 2017 May 21;3:24.
79. Chung DJ, Arif B, Odia Y, Siomin V. Chemotherapy-induced changes in tumor consistency can allow gross total resection of previously unresectable brainstem pilocytic astrocytoma. *Surg Neurol Int*. 2021 Jan 13;12:12.
80. Cuce F. Radiopaedia. 2024 [cited 2024 Jun 26]. Neuro-Behçet disease | Radiology Case | Radiopaedia.org. Available from: <https://radiopaedia.org/cases/neuro-behçet-disease-6>
81. De Cocker L. Pathology of the Posterior Fossa. *J Belg Soc Radiol*. 2022 Nov 18;106(1):117.
82. Du Y, Lu T, Huang S, Ren F, Cui G, Chen J. Somatic mutation landscape of a meningioma and its pulmonary metastasis. *Cancer Commun Lond*

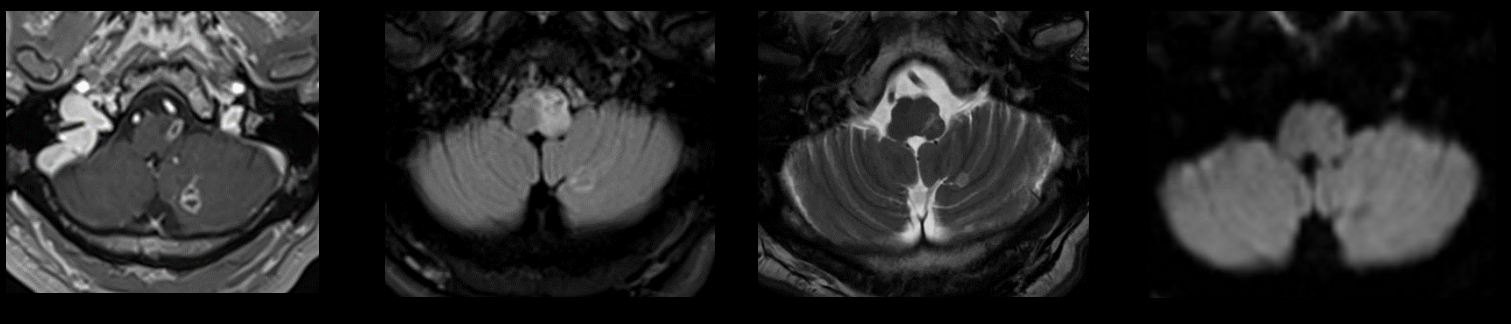
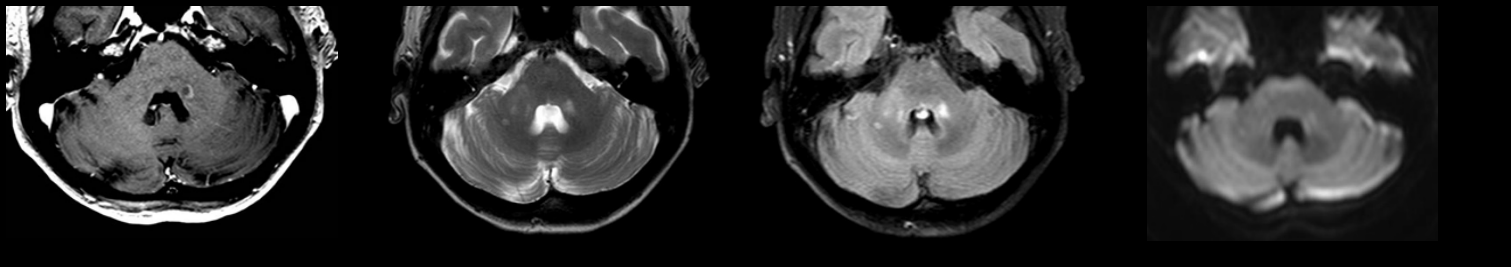
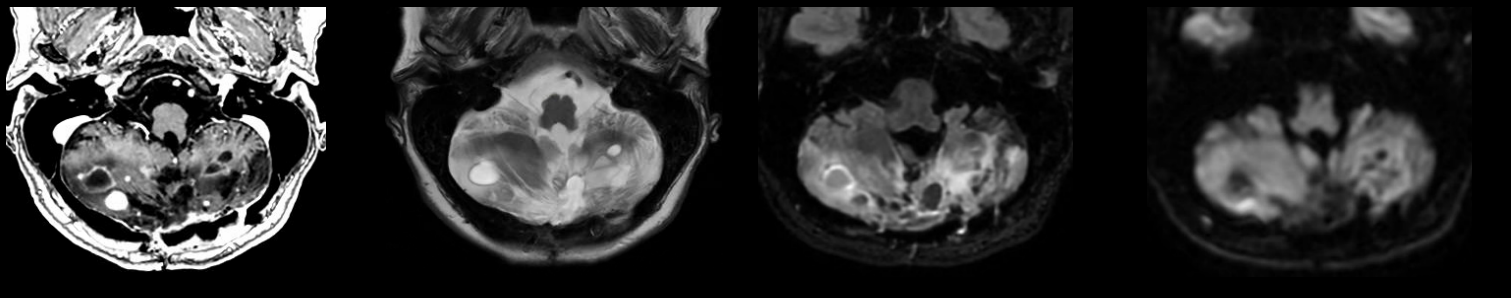
Engl. 4 mai 2018;38(1):16.

83. Duran-Peña A, Ducray F, Ramirez C, Bauchet L, Constans J, Grand S, et al. Adult Brainstem Glioma Differential Diagnoses: An MRI-based Approach in a Series of 68 Patients. *J Neurol*. 2022 Aug 1;269:1–14.
84. Einarsson HB, Thorvaldsen MON, Kehrer M, Harbo FSG, Hansen SGK, Munck DF, et al. A 26-year-old woman with brainstem abscess at third trimester of pregnancy: Case report. *Interdiscip Neurosurg*. 2021 Dec 1;26:101337.
85. Cure of a solitary abscess with antibiotic therapy | *Neurology* [Internet]. 2024 [cited 2024 Jun 26]. Available from: <https://www.neurology.org/doi/10.1212/WNL.46.5.1451>
86. Gaillard F. Radiopaedia. 2024 [cited 2024 Jun 26]. Cerebellar abscess | Radiology Case | Radiopaedia.org. Available from: <https://radiopaedia.org/cases/cerebellar-abscess>
87. Guzmán-De-Villoria JA, Fernández-García P, Ferreiro-Argüelles C. Differential Diagnosis of T2 Hyperintense Brainstem Lesions: Part 1. Focal Lesions. *Semin Ultrasound CT MRI*. 2010 Jun;31(3):246–59.
88. Hamamoto Filho PT, Zanini MA. Brainstem abscess of undetermined origin: microsurgical drainage and brief antibiotic therapy. *Sao Paulo Med J*. 2014;132(2):121–4.
89. Iwai Y, Ishibashi K, Nakanishi Y, Onishi Y, Nishijima S, Yamanaka K. Functional Outcomes of Salvage Surgery for Vestibular Schwannomas after Failed Gamma Knife Radiosurgery. *World Neurosurg*. 2016 Jun 1;90:385–90.
90. Januário G. Posterior Fossa Glioblastoma, Case Report, and Reviewed Literature. *Clin Cancer Investig J*. 2022;11(5):17–22.
91. Jha P. Radiopaedia. 2024 [cited 2024 Jun 26]. Cerebellar tuberculoma | Radiology Case | Radiopaedia.org. Available from: <https://radiopaedia.org/cases/cerebellar-tuberculoma>
92. Jung G, Ramina R. Vestibular Schwannomas: Diagnosis and Surgical Treatment. In 2019.
93. Kayaaslan BU, Akinci E, Bilen S, Gözel MG, Erdem D, Cevik MA, et al. Listerial rhombencephalitis in an immunocompetent young adult. *Int J Infect Dis IJID Off Publ Int Soc Infect Dis*. 2009 Mar;13(2):e65–67.
94. Khan S, Gupta S, Jain S, Singhanian S. Concurrent Pulmonary, Intracranial, Intramedullary Tuberculoma, and Their Response to Conservative Management. *Int J Recent Surg Med Sci*. 2019 Jan 22;4.
95. Lahiri S, Kumar M, Chickabasaviah Y, Kumari V, Raj P, Bharath R, et al. Cerebellar cryptococcoma due to *Cryptococcus gattii* VGI; a rare and first report from India. 2015 Jun 30;
96. Mokta J, Mahajan S, Machhan P, Mokta K, Patial R, Prashar B. Recurrent oculomotor nerve palsy: A rare presentation of neurocysticercosis. *Neurol India*. 2004 Oct 1;52:402.
97. Khurana N, Sharma P, Shukla R, Singh D, Vidhate M, Naphade PU. Midbrain neurocysticercosis presenting as isolated pupil sparing third cranial nerve palsy. *J Neurol Sci*. 2012 Jan 15;312(1):36–8.
98. Muzio BD. Radiopaedia. 2024 [cited 2024 Jun 26]. Glioblastoma IDH wild type (brainstem) | Radiology Case | Radiopaedia.org. Available from: <https://radiopaedia.org/cases/glioblastoma-idh-wild-type-brainstem>
99. Ngo T, Okabe A, Nguyen K, Tong A, Chang J, Lui F. Cryptogenic Pontine Abscess Treated With Stereotactic Aspiration: A Case Report. *Cureus*. 2023 Jul 6;15.
100. Nussbaum LA, Kallmes KM, Bellairs E, McDonald W, Nussbaum ES. De novo cavernous malformation arising in the wall of vestibular schwannoma following stereotactic radiosurgery: case report and review of the literature. *Acta Neurochir (Wien)*. 2019 Jan;161(1):49–55.
101. Patel SH, Saito YD, Li Z, Ramaswamy B, Stiff A, Kassem M, et al. A solitary brain metastasis as the only site of recurrence of HR positive, HER2 negative breast cancer: a case report and review of the literature. *J Med Case Reports*. 2021 Jan 7;15(1):4.
102. Pignotti F, Conforti G, Lauretti L, Pallini R, Fernandez E, D'Alessandris Q. Tuberculoma of the Posterior Fossa: A Neurosurgical Matter. In 2019 [cited 2024 Dec 7]. Available from: <https://www.semanticscholar.org/paper/Tuberculoma-of-the-Posterior-Fossa%3A-A-Neurosurgical-Pignotti-Conforti/16941123ad4ac1cd00c2eb081a891800a8cda4e3>
103. Ravikanth R, Majumdar P, Pinto D. Cystic Vestibular Schwannomas and Post-Gamma Knife Radiosurgery-Induced Necrosis of Vestibular Schwannomas: Report of Two Cases and Review of Literature. *Asian J Oncol*. 2020 Mar 9;6.
104. Razok A, Ali M, Shams A, Zahid M. Neurocysticercosis presenting with oculomotor nerve palsy: Case report and literature review. *IDCases*. 2023 Jan 1;32:e01788.
105. Salaskar AL, Hassaneen W, Keenan CH, Suki D. Intracranial tuberculoma mimicking brain metastasis. *J Cancer Res Ther*. 2015;11(3):653.
106. Sethi P, Treece J, Onweni C, Pai V, Rahman Z, Singh S. The Importance of a Complete Differential: Case Report of a Tuberculoma in a Patient without Pulmonary Involvement. *Cureus*. 2017 Jun 28;9.
107. Shimizu Y, Tsuchiya K, Fujisawa H. Nocardia paucivorans cerebellar abscess: Surgical and pharmacotherapy. *Surg Neurol Int*. 2019;10:22.
108. Shoap W, Hayden EA, Crabill GA. Persistent brainstem abscess requiring repeat microsurgical drainage: case report. *J Surg Case Rep*. 2021 Aug 31;2021(8):rjab376.
109. Sumer S, Koktekir E, Aktug Demir N, Akdemir G. Intracranial Giant Tuberculoma Mimicking Brain Tumor: A Case Report. *Turk Neurosurg*. 2014 Jan 1;25.
110. Tan CH. Flow Related Aneurysm in Hemangioblastoma and Literature Review of Hemorrhagic Rate and Management Strategy. *Neurosurg Cases Rev*. 2021 Apr 29;4(2):068.
111. Themes UFO. Radiology Key. 2015 [cited 2024 Jun 26]. Breast Cancer Metastases to the Neural Axis. Available from: <https://radiologykey.com/breast-cancer-metastases-to-the-neural-axis/>
112. Usman N, Jayasri G, MLP. Case report on cerebellar hemangioblastoma showing post contrast cyst wall enhancement on magnetic resonance imaging. *Med Sci*. 2023 Jan 7;27(131):1–6.
113. Verma S, Satapara J, Makada M, Bahri N. Pontine tuberculoma in a known case of tuberculosis. 2018 Sep 24;
114. Watts J, Box G, Galvin A, Brothie P, Trost N, Sutherland T. Magnetic resonance imaging of meningiomas: a pictorial review. *Insights Imaging*. 2014 Feb;5(1):113–22.
115. Zhang X, Katsakhyan L, LiVolsi VA, Roth JJ, Rassekh CH, Bagley SJ, et al. TP53 Mutation and Extraneural Metastasis of Glioblastoma: Insights From an Institutional Experience and Comprehensive Literature Review. *Am J Surg Pathol*. 2021 Nov 1;45(11):1516–26.
116. Zhenxing S, Yuan D, Sun Y, Yan P, Zuo H. Surgical resection of cerebellar hemangioblastoma with enhanced wall thickness: A report of two cases. *Oncol Lett*. 2015 Feb 10;9.
117. Inoue T, Katoh N, Aoyama H, Onimaru R, Taguchi H, Onodera S, et al. Clinical outcomes of stereotactic brain and/or body radiotherapy for patients with oligometastatic lesions. *Jpn J Clin Oncol*. 2010 Aug;40(8):788–94.

SUPPLEMENTAL FILES

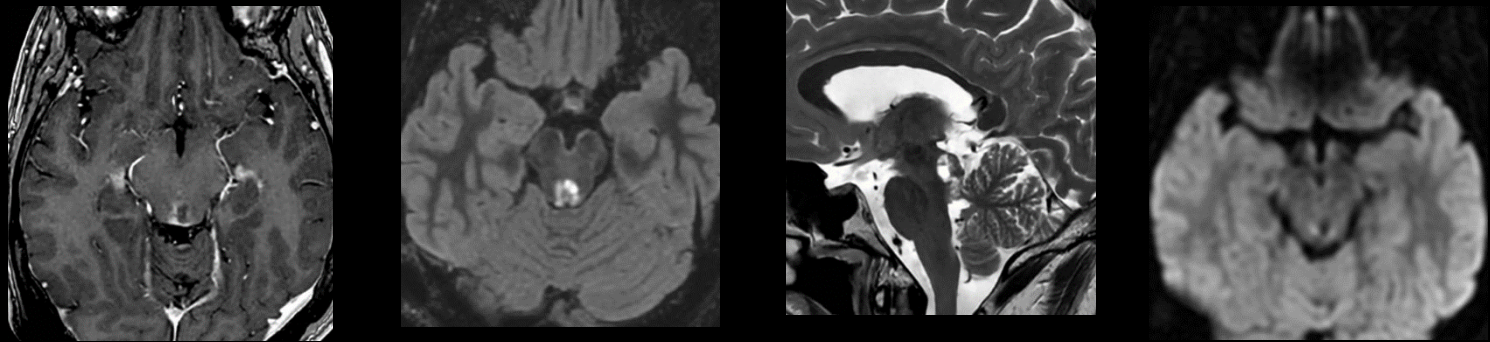
Supplementary Table 1: Institutional case series

Patients	T1-w post-Gd	FLAIR	T2-w	DWI	Diagnosis
1) F, 73 y History of chronic lymphocytic leukaemia					Richter's syndrome
2) M, 54 y History of posterior fossa surgery and irradiation for ependymoma. SUV max 2.9					Radionecrosis

<p>3) M, 57 y, Acute vertigo onset one week before MRI</p>		<p>Subacute stroke</p>
<p>4) F, 62 y Supratentorial lesions compatible with multiple sclerosis</p>		<p>Multiple sclerosis</p>
<p>5) F, 43 y History of Von Hippel- Lindau disease</p>		<p>Hemangioblastoma</p>

6) M, 39 y

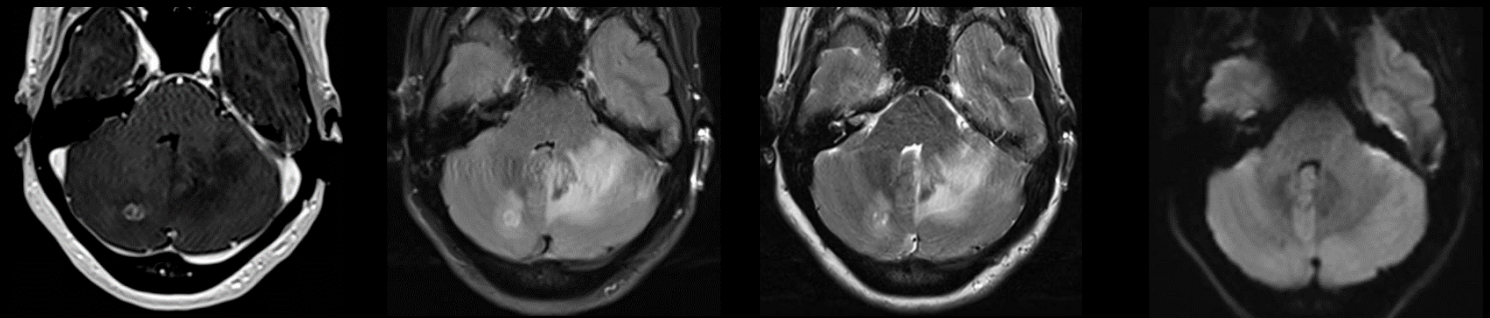
Progressive
headaches
evolving for
weeks due to
hydrocephalus



Pinealoblastoma

7) F, 48 y

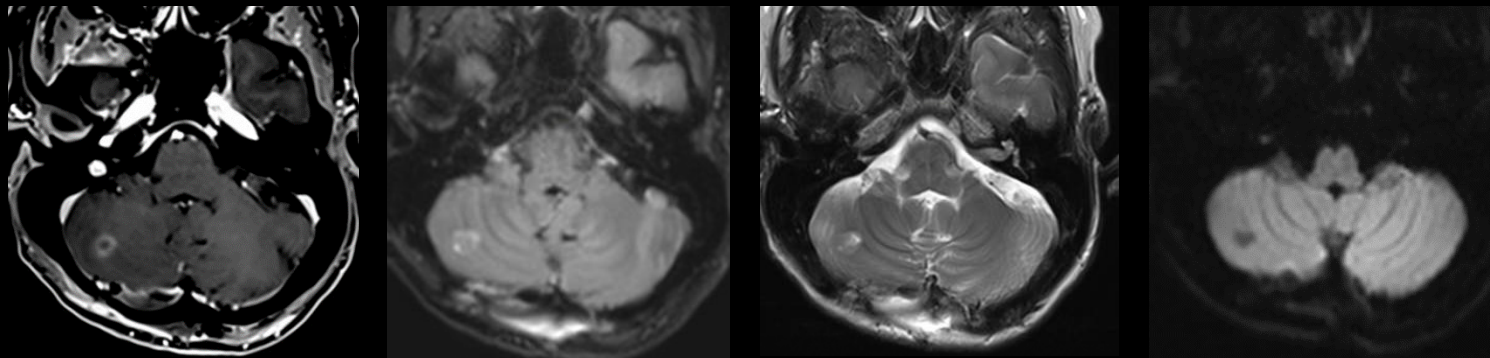
Suspect
pulmonary
nodule on
chest X-ray



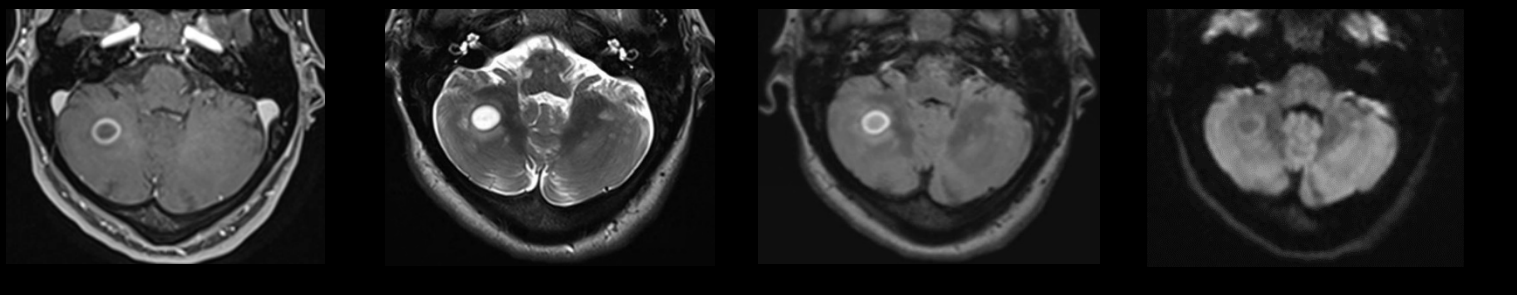
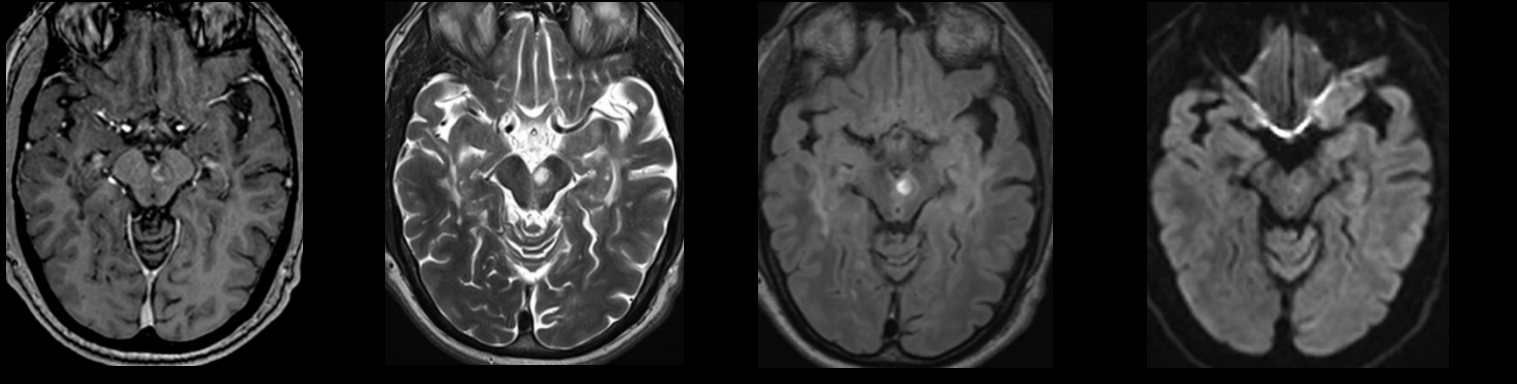
Metastasis (lung
adenocarcinoma)

8) F, 65 y

History of
metastatic
ovarian
carcinoma



Metastasis (ovarian
carcinoma)

<p>9) F, 24 y</p> <p>Supratentorial lesions compatible with multiple sclerosis</p>		<p>Multiple sclerosis</p>
<p>10) M, 50 y</p> <p>History of multiple sclerosis</p>		<p>Multiple sclerosis</p>

Abbreviations: PFREL, posterior fossa ring enhancing lesion; T1-w post-Gd, T1-weighted post gadolinium; T2-w, T2-weighted, DWI, diffusion weighted image; SUV max: maximum standardized uptake value

Supplementary Table 2: Literature review

No.	References	Ref No.	Type of etiology	Specific etiology	Sex	Age (years)	Country/ Ethnicity	Comorbidities	Clinical	Duration of symptoms to admission	Treatment	Outcome
1	Adachi et al., 1995	24	Infectious	Abscess	M	52	Japan	Cirrhosis	Fever, diplopia, left hemiparesis	3 days	Ventriculo-peritoneal shunt, imipenem, clastin and gentamicin	Mild left hemiparesis at 8 months
2	Alhamshari et al., 2015	25	Infectious	Abscess	M	77	USA (African American)	Hypertension	Nausea, vomiting, vertigo, ataxia, lethargy	3 days	Empiric vancomycin, meropenem, corticosteroids	Rehabilitation
3	Alharbi et al., 2021	26	Infectious	Tuberculosis	M	67	Saudi-Arabia	No	Nausea, vomiting, instability, ataxia	15 days	Surgical resection, antituberculosis therapy	Mild cerebellar dysfunction at 6 months
4	Arif et al., 2020	27	Infectious	Tuberculosis	M	65	Pakistan	Hypertension	Anorexia, fever, headache, confusion	2 months	Dexanethasone and antituberculosis therapy	Asymptomatic
5	Besada et al., 2010	28	Tumoral	Metastasis (adenocarcinoma, lung cancer)	M	58	Argentina	NA	Headache, cough	NA	Surgical resection	NA
6	Bhattacharjee et al., 2012	29	Infectious	Tuberculosis	F	48	Turkey	No	Headache, nystagmus, ataxia	8 weeks	Surgical resection, antituberculosis therapy	Alive
7	Capone et al., 2021	30	Infectious	Tuberculoma	M	41	Yemen	NA	Headaches and night sweat	3 months	Surgical resection, antituberculosis therapy	Asymptomatic
8	Chin et al., 2020	31	Inflammatory	Tuberculosis-IRIS	M	57	Malaysia	Hepatitis C, cirrhosis	Hemiparesis, slurred speech	5 days	Surgical resection, antituberculosis therapy	Recovered at 7 months
9	de Almeida et al., 2020	32	Infectious	Fungal disease (Histoplasma capsulatum)	M	23	Brasil	NA	Intracranial hypertension, ataxia, diplopia, dysarthria	NA	Ventriculo-peritoneal shunt, amphotericin B	Nystagmus, dysarthria and instability at 13 years
10	De Keersmaecker et al., 2024	33	Tumoral	Metastasis (small cell lung carcinoma)	F	76	Belgium	Uretral cancer, hypertension, hypercholesterolemia	Tiredness, dizziness and headaches	2 months	Radiotherapy	Deceased
11	Feizi et al., 2021	34	Inflammatory	Neurosarcoidosis	F	47	African American	Hypertension	Hemiparesis	NA	Corticosteroids	Improvement of hemiparesis
12	Fereydonyan et al., 2019	35	Tumoral	Squamous cell carcinoma (from an epidermoid cyst)	M	30	Iran	NA	Headache, nausea, vomiting	NA	Surgical resection and radiotherapy	Recovered at 2 years
13	Gottlieb et al., 2015	36	Infectious	Tuberculosis	M	46	Mexican	Alcoholism	Diplopia (cranial nerve III palsy)	5 days	Prednisone, antituberculosis therapy	Improvement of diplopia
14	Goto et al., 2015	2	Infectious and tumoral	Abscess within metastasis	M	56	Japan	Aortic aneurysm, bile duct cancer	Instability, ataxia	NA	Surgical resection and stereotaxic radiosurgery	Asymptomatic at 3 months
15	Heo et al., 2008	37	Inflammatory	Neuro-Behçet	M	47	Korea	NA	Hemiparesis, dysarthria, headache, vomiting	5 days	High dose steroid therapy	NA
16	Imoto et al., 2002	38	Inflammatory	Neuro-Behçet	M	50	Japan	Psychoneurosis	Hemiparesis, dysarthria	2 weeks	Corticosteroid pulse therapy	Improvement of hemiparesis
17	Inoue et al., 2016	117	Tumoral	Glioblastoma	M	27	Japan	Grade II astrocytoma	Headache, nausea, cerebellar symptoms	NA	Surgical resection, ventriculo-peritoneal shunt, radio-chemotherapy	Deceased
18	Jongeling et Pisapia, 2013	39	Infectious	Tuberculosis	M	21	Ecuador	NA	Headache, fever, meningism	5 days	Antituberculosis therapy	Deceased
19	Jorge et al., 2017	40	Infectious	Fungal disease (Neuroparacoccidio mycosis)	M	49	Latin America	Smoking, alcoholism, brain trauma	Headache, dysidiadochokinesia	3 months	Surgical resection	NA
20	Kim et Kim, 2008	41	Tumoral	Epidermoid cyst	M	72	Korea	NA	Hemiparesis, dysphagia, hemifacial numbness	2 months	Surgical resection and radiotherapy	Improvement of hemiparesis and dysphagia

21	Kong et al., 2006	42	Tumoral	Metastasis (adenocarcinoma, lung cancer)	M	74	Australia	Smoking, hypertension, COPD	Personality change, confusion and headache	6 weeks	NA	NA
22	Lakra et al., 2023	43	Tumoral	Metastasis (adenocarcinoma, colorectal cancer)	M	29	Caucasian	Asthma and colorectal cancer	Altered mental status	NA	Surgical resection	Deceased
23	Lath et Rajshekhar, 1998	44	Infectious	Neurocysticercosis	F	32	India	NA	Headache and transient oculoparesis	6 months	Symptomatic	Asymptomatic
24	Lee et al., 2011	45	Infectious	Tuberculosis	F	23	Somalia	NA	Headache, nausea, vomiting	4 months	Surgical resection, antituberculosis therapy, corticosteroids	Asymptomatic at 9 months
25	Li et al., 2013	46	Infectious	Sparganosis	M	36	China	NA	Seizures, hemiparesis	17 years	NA	NA
26	Li et al., 2022	1	Tumoral	Hemangioblastoma	F	33	China	NA	Headache, visual loss, instability, facial numbness	1 week	Surgical resection	Asymptomatic after surgery and at 2 years
27	Lyons et al., 2013	47	Infectious	Tuberculoma	F	43	USA	NA	Headache, dizziness, hemiparesis	1 month	Dexanethasone and antituberculosis therapy	Asymptomatic at 6 months
28	Mandapat et al., 2011	48	Infectious	Abscess (Streptococcus salivarius)	F	55	USA	No	Headache, ataxia, hemiparesis, dysphagia, ptosis, cranial nerve VI palsy	3 days	Surgical drainage, ceftriaxone	Dysesthesia at 6 months
29	Maruya et al., 2009	49	Tumoral	Pineal region tumor (germinoma)	M	29	Japan	NA	Diplopia, upward gaze nystagmus	8 months	Chemotherapy, radiotherapy	Asymptomatic at 5 years
30	Matsumoto et al., 1998	50	Tumoral	Metastasis (adenocarcinoma)	M	46	Japan	NA	Hemisensory disturbance and hemiparesis	2 months	Brachytherapy, chemotherapy	Asymptomatic at 18 months
31	Medina-Flores et al., 2003	51	Infectious	Abscess (Listeria)	F	59	USA	Hypertension, diabetes, coronary artery disease, dental implants	Diplopia, headache, central facial palsy	1 week	Ampicillin, trimethoprim, sulfamethoxazole, corticosteroids	Facial numbness
32	Naphade et al., 2012	52	Infectious	Neurocysticercosis	F	45	India	NA	Bilateral ptosis	4 days	Steroids, albendazole	Asymptomatic at 3 months
33	Niu et al., 2017	53	Infectious	Abscess (Aggregatibacter aphrophilus)	M	28	USA	NA	Headache	6 months	Vancomycin, ceftriaxone	Asymptomatic at 4 months
34	O'Callaghan et al., 2012	54	Infectious	Abscess (Listeria monocytogenes)	F	25	Ireland	No	Headache, nausea, vomiting, hemianesthesia	4 days	Amoxicillin, gentamycin	Asymptomatic at 1 month
35	Otero et al., 2022	55	Tumoral	Schwannoma of the XIth nerve	M	61	Spain	Hypertension, diabetes, smoking, dyslipidemia	Instability, dysmetria, vomiting	3 months	Surgical resection	Deceased
36	Parekh et al., 2014	56	Infectious	Tuberculosis	M	82	Yemen	Prostate cancer, atrial fibrillation, diabetes, cirrhosis	Altered mental status	NA	Antituberculosis therapy	Deceased
37	Pekova et al., 2021	57	Infectious	Toxoplasma gondii	M	23	Bulgaria	No	Fever, confusion, dysarthria, ataxia, headache, meningism, hemiparesis	3 weeks	Ceftriaxone, amikacin, mannitol, dexamethasone, antituberculosis therapy	Deceased
38	Raheja et al., 2016	58	Tumoral	Squamous cell carcinoma (from an epidermoid cyst)	F	54	USA	NA	Altered mental status	Few weeks	Surgery	Declined treatment
39	Raval et al., 2012	59	Infectious	Neurocysticercosis	M	31	Asian	NA	Vision loss	6 months	Albendazole and steroids	Alive
40	Sankar et al., 2021	60	Infectious	Tuberculosis	F	56	India	No	Bilateral ptosis	1 month	Dexamethasone, antituberculosis therapy	Asymptomatic at 1 month
41	Shaikh et al., 2019	61	Tumoral	Squamous cell carcinoma (from a dermoid cyst)	M	32	Pakistan	NA	Headache, vertigo	3 weeks	Ventriculoperitoneal shunt and surgical excision	NA

42	Shih et al., 1993	62	Tumoral	Metastasis (bronchogenic carcinoma)	M	71	USA	Smoking, COPD, hypertension, alcoholism	Dizziness, nausea, vomiting, gait instability	3 weeks	Craniotomy, tumor resection, radiotherapy	NA
43	Shrestha et al., 2024	63	Infectious	Abscess	F	63	USA	Chronic suppurative otitis media and cholesteatoma	Gait difficulty and ataxia, hearing loss, right facial palsy	NA	Surgical needle aspiration and radical mastoidectomy	Hearing loss
44	Sinha et al., 2010	64	Infectious	Tuberculosis	M	29	India	No	Fever, headache, seizures	NA	Dexamethasone, antituberculosis therapy	Asymptomatic
45	Song et al., 2010	65	Infectious	Neurocysticercosis	M	68	Korea	No	Claude's syndrome (ipsilateral cranial nerve III palsy with contralateral hemiataxia)	2 days	Albendazole, methylprednisolone	Asymptomatic at one week
46	Suzuki et al., 2019	66	Infectious	Granulomatous amoebic encephalitis	M	68	Japan	No	Focal epilepsy	NA	Surgical resection	Deceased
47	Taylor et al., 2008	67	Tumoral	Dysembryoplastic neuroepithelial tumor	F	34	USA	No	Headache, vertigo, altered consciousness, truncal ataxia	5 months	Surgical resection	Asymptomatic at 9 months
48	Tanaka et al., 2020	68	Infectious	Abscess (Nocardia beijingensis)	M	68	Japan	No	Loss of appetite, headache, vomiting, progressive disturbance of consciousness.	1 month	Methylprednisolone, meropenem and trimethoprim/sulfamethoxazole	Confusion and irritability, discharged to another hospital
49	Toshikuni et al., 2007	69	Tumoral	Metastasis (hepatocellular carcinoma)	M	78	Japan	Cirrhosis	Hemiparesis	1 month	Whole-brain radiotherapy	Alive at 12 months, resolution of hemiparesis
50	Tsutsumi et al., 2001	70	Tumoral	Metastasis (lung adenocarcinoma)	M	56	Japan	Lung cancer (adenocarcinoma)	Hearing disturbance, ataxic gait, dysmetria	NA	Surgical resection, gamma knife	Persistent hearing disturbance, improvement of ataxia
51	Uchino et al., 2006	71	Tumoral	Pineal region tumor (cystic germinoma)	M	22	Japan	NA	Diplopia, headache	NA	Chemotherapy, radiotherapy	NA
52	Ueno et al., 2014	72	Inflammatory	CLIPPERS	M	58	Japan	NA	Dysarthria, gait disturbance	6 months	Methylprednisolone	Asymptomatic at 6 months
53	Utsuki et al., 2012	73	Tumoral	Pilocytic astrocytoma	F	18	Japan	NA	Visual disturbance	2 months	Surgical resection	NA
54	Wang et al., 2015	74	Tumoral	Gliosarcoma	M	28	China	NA	Headache, vomiting, gait instability	3 months	Surgical resection	NA
55	Yasuda et al., 2012	14	Inflammatory	Neuro-Behçet	M	56	Japan	NA	Paresis and dysesthesia	NA	Corticosteroids	NA
56	Yiu et Lessell, 2012	75	Tumoral	Metastasis (melanoma)	M	60	USA	Diabetes, COPD, hyperlipidemia	Visual disturbance, gait instability	2 weeks	Dexamethasone, stereotactic radiosurgery	Deceased

IRIS Immune reconstitution inflammatory syndrome, *NA* Not Available, *COPD* Chronic obstructive pulmonary disease, *CLIPPERS* Chronic Lymphocytic Inflammation with Pontine Perivascular Enhancement Responsive to Steroids

No.	References	Ref No.	Number of lesions in the posterior fossa	Size (cm)	Location	DWI	FLAIR	T1-weighted images	T2-weighted images	Biopsy/ Resection	CSF	Chest
1	Adachi et al., 1995	24	1	NA	Brainstem	NA	NA	Hyposignal	NA	NA	1301/μL WBC (polynuclear predominance)	Interstitial pneumonia
2	Alhamshari et al., 2015	25	Multiple	Largest is 1.2×2.0	Cerebellum	NA	NA	NA	NA	NA	12 /μL WBC (neutrophilic predominance)	Prominent pulmonary arteries
3	Alharbi et al., 2021	26	1	2.0 x 2.3 x 2.3	Cerebellum	NA	Hypersignal for the rim, hyposignal for the center	NA	Hypersignal for the rim, hyposignal for the center	Done	NA	Bilateral pulmonary nodules, reactive lymph nodes
4	Arif et al., 2020	27	Multiple	NA	Brainstem, Cerebellum	No restriction	No restriction	Iso to hyposignal	Hyposignal	NA	250 /μL WBC (lymphocytic predominance). Positive for	Negative

											Mycobacterium tuberculosis	
5	Besada et al., 2010	28	1	NA	Cerebellar hemisphere	Hypersignal	NA	NA	Hyperintense mass, peripheral edema	Done	NA	Parahilar nodule right superior lung
6	Bhattacharjee et al., 2012	29	1	NA	Cerebellar hemisphere	NA	NA	NA	Hypersignal for the rim, isosignal for the center	Done	NA	Negative
7	Capone et al., 2021	30	1	2.5 x 2.0	Cerebellar hemisphere	NA	NA	NA	Hyposignal	Done	NA	Calcified lymph nodes
8	Chin et al., 2020	31	Multiple	NA	Cerebellar hemispheres and vermis	NA	NA	NA	NA	Done	Negative for Mycobacterium tuberculosis	Miliary tuberculosis
9	de Almeida et al., 2020	32	Multiple	NA	Cerebellum, brainstem	NA	NA	NA	NA	NA	Lymphocytic pleiocytosis, culture positive for fungus (Histoplasma)	NA
10	De Keersmaecker et al., 2024	33	Multiple	NA	Brainstem, Cerebellum	No restriction	Hypersignal for the rim, hyposignal for the center	NA	NA	NA	NA	Nodular lesions and adenopathies
11	Feizi et al., 2021	34	1	NA	Pons	NA	Hypersignal for the rim, hyposignal for the center	NA	NA	Done	NA	Negative
12	Fereydonyan et al., 2019	35	1	NA	Cerebellar peduncle	NA	NA	Isosignal	Isosignal	Done	NA	NA
13	Gottlieb et al., 2015	36	1	1.1 x 1.0 x 1.5	Central midbrain	NA	NA	NA	NA	NA	NA	Calcified granuloma, reticulonodular opacities
14	Goto et al.,	2	1	NA	Cerebellar hemisphere	Hypersignal	NA	Hyposignal	Hypersignal	Done	NA	NA
15	Heo et al., 2008	37	1	NA	Pons	Hypersignal	NA	NA	NA	Done	NA	NA
16	Imoto et al., 2002	38	Multiple	NA	Brainstem	NA	NA	Hyposignal	Hypersignal with areas of hyposignal	Done	14 /μL WBC	NA
17	Inoue et al., 2016	117	1	NA	Cerebellar hemisphere	NA	NA	Hyposignal	Hypersignal	Done	NA	NA
18	Jongeling et Pisapia, 2013	39	Multiple	NA	Cerebellum	NA	NA	NA	NA	NA	WBC 85/μL (lymphocytic predominance) then control at 250/μL (lymphocytic predominance). Positive for Mycobacterium tuberculosis	Dense consolidations, diffuse micronodular opacities
19	Jorge et al., 2017	40	1	NA	Cerebellar hemisphere	Hypersignal	Perilesional edema, hyposignal for the rim, hypersignal for the center	Hypersignal for the rim, hyposignal for the center	Perilesional edema, hyposignal for the rim, hypersignal for the center	Done	NA	Pulmonary nodules
20	Kim et Kim, 2008	41	1	NA	Cerebellar peduncle	Hypersignal	NA	NA	NA	Done	NA	Negative
21	Kong et al., 2005	42	Multiple	NA	Supra- and infratentorial	NA	NA	Hyposignal	Hypersignal for the rim, hyposignal for the center	Done	NA	Spiculated lung nodule
22	Lakra et al., 2023	43	1	0.9 x 0.8 x 0.8	Anterolateral medulla oblongata	NA	Hypersignal for the rim, hyposignal for the center, perilesional edema	NA	NA	Done	NA	NA
23	Lath et Rajshekhar, 1998	44	1	<2.0	Dorsal ponto-medullary junction	NA	NA	Hyposignal	Hyposignal for the rim, hypersignal for the center, hyposignal scolex	NA	Negative	NA
24	Lee et al., 2011	45	1	NA	Cerebellar hemisphere	NA	NA	NA	NA	Done	Positive for Mycobacterium tuberculosis	NA

25	Li et al., 2013	46	2	NA	Cerebellar hemisphere	NA	NA	NA	NA	NA	NA	NA
26	Li et al., 2022	1	2	3.9 × 3.6 × 3.4 and 2.1 × 2.0 × 1.5	Cerebellar hemisphere	NA	NA	Uneven signal intensities	Uneven signal intensities	Done	NA	NA
27	Lyons et al., 2013	47	1	2.9 x 2.7 x 2.5	Pons	No restriction	NA	Hyposignal	Hypersignal for the rim, hyposignal for the center	NA	Cryptococcal antigen negative	Adenopathies and apical lung scarring
28	Mandapat et al., 2011	48	1	2.6 x 2.0 x 1.9	Pons	Hypersignal	Hyposignal	Hyposignal	NA	Done	Positive for Streptococcus salivarius	NA
29	Maruya et al., 2009	49	1	NA	Thalamo-mesencephalic junction	NA	NA	NA	NA	Done	NA	NA
30	Matsumoto et al., 1998	50	1	1.0 x 2.0	Peduncle of the midbrain	NA	NA	NA	Hypersignal	Done	NA	Lung cancer
31	Medina-Flores et al., 2003	51	1	1.3 x 1.3 x 1.5	Cerebral peduncle	NA	NA	NA	Hypersignal	Done	NA	NA
32	Naphade et al., 2012	52	1	< 2.0	Dorsal midbrain	NA	NA	NA	NA	NA	Positive ELISA IgM cysticercus	NA
33	Niu et al., 2017	53	1	1.0 x 0.9	Midbrain tectum	Hypersignal	Hypersignal	NA	NA	NA	WBC 482/μL (lymphocytic predominance), culture positive for A. aphrophilus.	NA
34	O'Callaghan et al., 2012	54	Multiple	NA	Brainstem and upper cervical cord	NA	NA	NA	Hypersignal	NA	WBC 595 /μL (98% lymphocytes) Presence of plasma cells. Then control at 68 WBC/μL. PCR positive for Listeria monocytogenes	NA
35	Otero et al., 2022	55	1	3.5 x 3.8 x 4.5	Cerebellopontine angle	NA	NA	NA	NA	Done	NA	NA
36	Parekh et al., 2014	56	Multiple	NA	Cerebellar hemisphere	NA	NA	NA	NA	Done	NA	Negative
37	Pekova et al., 2021	57	Multiple	NA	Brainstem and cerebellum	NA	Hypersignal for the rim, hyposignal for the center	NA	Hypersignal for the rim, hyposignal for the center	NA	WBC 96 /μL (97% lymphocytes)	Negative
38	Raheja et al., 2016	58	1	NA	Dorsal midbrain	Hypersignal	NA	NA	NA	Done	Lymphocytic pleocytosis	Negative
39	Raval et al., 2012	59	1	NA	Cerebellar hemisphere	NA	NA	NA	NA	NA	NA	NA
40	Sankar et al., 2021	60	1	0.9 x 0.85	Medial midbrain	No restriction	Isosignal for the rim, hypersignal for the center	Isosignal	Isosignal for the rim, hypersignal for the center	NA	Normal	Lymphadenopathy, fibrocalcific opacities in apices
41	Shaikh et al., 2019	61	1	5.0 x 4.8	Cerebellum	NA	NA	Hyposignal	Hypersignal	Done	NA	NA
42	Shih et al., 1993	62	Multiple	Largest is 2.8	Cerebellum	NA	NA	NA	NA	Done	NA	Apical mass
43	Shrestha et al., 2024	63	1	1.9 x 2.1 x 2.2	Cerebellar peduncle	Hypersignal	Hypersignal	Hyposignal	NA	Done	WBC 12 /μL	NA
44	Sinha et al., 2010	64	Multiple	NA	NA	NA	NA	NA	NA	NA	NA	NA
45	Song et al.,	65	1	NA	Midbrain	NA	Hypersignal	NA	NA	NA	3 mononuclear cell /μL. ELISA for	NA

	2010				tegmentum						an anticysticercal antibody positive	
46	Suzuki et al., 2019	66	Multiple	NA	Brainstem	NA	Hypersignal	Hyposignal	Hypersignal	Done	High $\beta 2$ -microglobulin level	Negative
47	Taylor et al., 2008	67	4	1 x 1 and 0.8 x 0.8	Cerebellar vermis and midline	NA	NA	Hyposignal	Hypersignal	Done	NA	NA
48	Tanaka et al., 2020	68	Multiple	NA	Whole brain, brain stem, cervical spinal cord	NA	NA	NA	NA	Done	WBC 19 / μ L (mononuclear 52 %; polymorphonuclear 48 %)	Atelectasis
49	Toshikuni et al., 2007	69	Multiple	< 2.0	Cerebellum	NA	NA	Hyposignal	Hypersignal	NA	NA	Negative
50	Tsutsumi et al., 2001	70	1	1.2 x 1.3 x 1.5	Ventral left middle cerebellar peduncle	NA	NA	Hyposignal	Hypersignal, peritumoral edema	Done	NA	Negative
51	Uchino et al., 2006	71	1	NA	Midbrain	NA	NA	Hyposignal	NA	Done	NA	NA
52	Ueno et al., 2014	72	Multiple	NA	Pons, brachium pontis, midbrain	NA	NA	NA	NA	NA	Normal	Negative
53	Utsuki et al., 2012	73	1	NA	Vermis	NA	NA	NA	NA	Done	NA	NA
54	Wang et al., 2015	74	1	2.2 x 3.6 x 3.5	Middle cerebellar peduncle	NA	NA	Hyposignal	NA	Done	NA	NA
55	Yasuda et al., 2012	14	1	NA	Pontine base	Hypersignal	Hyposignal for the rim, hypersignal for the center	NA	NA	NA	Mononuclear pleiocytosis	NA
56	Yiu et Lessell, 2012	75	1	NA	Midbrain	NA	Hypersignal	NA	NA	NA	NA	Nodule

Abbreviations: NA, Not Available; Tuberculosis-IRIS, Tuberculosis-immune reconstitution inflammatory syndrome; COPD, Chronic obstructive pulmonary disease; CLIPPERS, chronic lymphocytic inflammation with pontine perivascular enhancement responsive to steroids; WBC White blood count, ELISA Enzyme-linked immunosorbent assay

Supplementary Table 3: Patients' characteristics

Variables	Overall (n=56)	Infectious group (n=29)	Inflammatory group (n=6)	Tumoral group (n=21)
Demographic characteristics				
Mean age in years (range)	47.9 (18-82)	47.5 (21-82)	52.5 (47-58)	47.0 (18-78)
Female sex, n (%)	16 (28.6)	10 (34.5)	1 (16.7)	5 (23.8)
Male sex, n (%)	40 (71.4)	19 (65.5)	5 (83.3)	16 (76.2)
Comorbidities, n (%)				
Reported healthy	11 (19.6)	10 (34.5)	0 (0)	1 (4.8)
Hypertension	8 (14.3)	3 (10.3)	1 (16.7)	4 (19.0)
Cancer	7 (12.5)	3 (10.3)	0 (0)	4 (19.0)
Alcoholism	3 (5.3)	2 (6.9)	0 (0)	1 (4.8)
Cirrhosis	4 (7.1)	2 (6.9)	1 (16.7)	1 (4.8)
COPD	3 (5.3)	0 (0)	0 (0)	3 (14.3)
Diabetes	4 (7.1)	2 (6.9)	0 (0)	2 (9.5)
Smoking	4 (7.1)	1 (3.4)	0 (0)	3 (14.3)
Clinical characteristics				
<i>Duration of symptoms, n (%)</i>				
Less than one week	10 (17.9)	8 (27.6)	2 (33.3)	0 (0)
One week to one month	13 (23.2)	6 (20.7)	1 (16.7)	6 (28.6)
More than one month	19 (33.9)	9 (31.0)	1 (16.7)	9 (42.8)
NA	14 (25.0)	6 (20.7)	2 (33.3)	6 (28.6)
<i>Symptoms, n (%)</i>				
Headache	26 (46.4)	15 (51.7)	1 (16.7)	10 (47.6)
Instability	19 (33.9)	9 (31.0)	1 (16.7)	9 (42.8)
Visual disturbances	16 (28.6)	11 (37.9)	0 (0)	5 (23.8)
Hemiparesis	13 (23.2)	5 (17.2)	5 (83.3)	3 (14.3)
Nausea	11 (19.6)	5 (17.2)	1 (16.7)	5 (23.8)
Imaging and laboratory features				
Multiple PFREL, n (%)	20 (35.7)	11 (37.9)	3 (50)	6 (28.6)
Median size in cm (range, n)	2.0 (0.9-5.0, n=22)	2.0 (0.9-2.9, n=12)	NA	2.4 (0.9-5.0, n=10)
<i>Chest imaging, n (%)</i>				
Normal	11 (19.6)	5 (17.2)	2 (33.3)	4 (19.0)
Abnormal	17 (30.4)	10 (34.5)	1 (16.7)	6 (28.6)
NA	28 (50)	14 (48.3)	3 (50)	11 (52.4)
<i>CSF, n (%)</i>				
Normal	5 (8.9)	3 (10.3)	2 (33.3)	0 (0)
Abnormal	18 (32.1)	15 (51.7)	2 (33.3)	1 (4.8)
NA	33 (58.9)	11 (37.9)	2 (33.3)	20 (95.2)
Biopsy/Resection done, n (%)	34 (60.7)	12 (41.4)	4 (66.7)	18 (85.7)
Etiology subgroup, n (%)				
		Abscess – 9 (31.0)	Tuberculosis-IRIS – 1 (16.7)	DNET – 1 (4.8)
		Fungal disease – 2 (6.9)	Neurosarcoidosis – 1 (16.7)	High grade glioma – 2 (9.5)
		Granulomatous amoebic encephalitis – 1 (3.4)	Neuro-Behçet – 3 (50)	Hemangioblastoma – 1 (4.8)
		Neurocysticercosis – 4 (13.8)	CLIPPERS – 1 (16.7)	Metastasis – 9 (42.8)
		Sparganosis – 1 (3.4)		Piloeytic astrocytoma – 1 (4.8)
		Toxoplasma gondii – 1 (3.4)		Pineal Region Tumor – 2 (9.5)
		Tuberculosis – 11 (37.9)		Lower cranial nerve schwannoma – 1 (4.8)
				Epidermoid cyst (or its transformation into squamous cell carcinoma) – 3 (14.3)
				Dermoid cyst (or its transformation into squamous cell carcinoma) – 1 (4.8)
Outcome, n (%)				
NA	11 (19.6)	2 (6.9)	2 (33.3)	7 (33.3)
Resolution	20 (35.7)	12 (41.4)	2 (33.3)	6 (28.6)
Residual symptoms	16 (28.6)	11 (37.9)	2 (33.3)	3 (14.3)
Died	9 (16.1)	4 (13.8)	0 (0)	5 (23.8)

NA Not Available, COPD Chronic obstructive pulmonary disease, PFREL posterior fossa ring-enhancing lesion, CSF Cerebrospinal fluid, IRIS Immune reconstitution inflammatory syndrome, CLIPPERS Chronic Lymphocytic Inflammation with Pontine Perivascular Enhancement Responsive to Steroids, DNET dysembryoplastic neuroepithelial tumor

Supplementary Table 4: Additional cases of PFREL

Case number	Diagnosis	References	Ref number
1	Abscess	Almeida et al., 2018	76
2	Metastasis	Byrne et al., 2020	77
3	Tuberculoma	Chan et al. 2021	21
4	Neurocysticercosis	Chowdury et al., 2017	78
5	Pilocytic astrocytoma	Chung et al., 2021	79
6	Behçet disease	Cuce et al., 2024	80
7	Abscess	De Cocker., 2022	81
8	Metastasis	Du et al., 2018	82
9	Metastasis	Duran-Pena et al., 2022	83
10	Behçet disease	Duran-Pena et al., 2022	83
11	Abscess	Einarsson et al., 2021	84
12	Abscess	Feraco et al., 2020	16
13	Abscess	Feraco et al., 2020	16
14	Abscess	Fulgham et al., 1996	85
15	Abscess	Gaillard et al., 2010	86
16	Multiple sclerosis	Guzmán-De-Villoria et al., 2010	87
17	Abscess	Hamamoto Filho et al., 2014	88
18	Vestibular schwannoma	Iwai et al., 2016	89
19	Glioblastoma	Januario, 2022	90
20	Tuberculoma	Jha, 2024	91
21	Vestibular schwannoma	Jung et al., 2019	92
22	Abscess	Kayaaslan et al., 2009	93
23	Tuberculoma	Khan et al., 2019	94
24	Neurocysticercosis	Khurana et al., 2012	97
25	Cryptococcoma	Lahiri et al., 2015	95

26	Neurocysticercosis	Mokta et al., 2004	96
27	Glioblastoma	Muzio., 2017	98
28	Abscess	Ngo et al. 2023	99
29	Vestibular schwannoma	Nussbaum et al., 2018	100
30	Abscess	Patel et al., 2021	101
31	Tuberculoma	Pignotti et al., 2019	102
32	Vestibular schwannoma	Ravikanth et al., 2020	103
33	Neurocysticercosis	Razok et al., 2023	104
34	Tuberculoma	Sadashiva et al., 2017	18
35	Tuberculoma	Sadashiva et al., 2017	18
36	Tuberculoma	Sadashiva et al., 2017	18
37	Tuberculoma	Salaskar et al., 2015	105
38	Tuberculoma	Sethi et al., 2017	106
39	Abscess	Shimizu et al., 2019	107
40	Abscess	Shoap et al., 2021	108
41	Tuberculoma	Sumer et al., 2014	109
42	Lymphoma	Sutherland et al., 2012	22
43	Hemangioblastoma	Tan et al., 2021	110
44	Metastasis	2015	111
45	Hemangioblastoma	Usman et al., 2023	112
46	Tuberculoma	Verma et al., 2018	113
47	Meningioma	Watts et al., 2014	114
48	MOG antibody-associated disease	Zhang et al., 2021	115
49	Hemangioblastoma	Zhenxing et al., 2015	116
50	Hemangioblastoma	Zhenxing et al., 2015	116

Abbreviations: PFREL, posterior fossa ring enhancing lesion; MOG antibody-associated disease, Myelin oligodendrocyte glycoprotein antibody-associated disease.

Supplementary Table 5: PFREL etiologies

Etiology	Number of patients (n = 116)	Percentage
Abscess	23	19,83%
Tuberculoma	22	18,97%
Metastasis	15	12,93%
Neurocysticercosis	8	6,90%
Hemangioblastoma	6	5,17%
Neuro-Behçet	5	4,31%
High grade glioma	4	3,45%
Multiple sclerosis	4	
Vestibular schwannoma	4	
Epidermoid cyst (or its transformation into squamous cell carcinoma)	3	2,59%
Pineal region tumor	3	1,72%
Fungal disease	2	
Pilocytic astrocytoma	2	
CLIPPERS	1	0,86%
Dermoid cyst (or its transformation into squamous cell carcinoma)	1	
Dysembryoplastic Neuroepithelial tumor	1	
Granulomatous amoebic encephalitis	1	
Lower cranial nerve schwannoma	1	

Lymphoma	1
Meningioma	1
MOG antibody-associated disease	1
Neurosarcoidosis	1
Radionecrosis	1
Richter's syndrome	1
Sparganosis	1
Subacute stroke	1
Tuberculosis-IRIS	1
Toxoplasmosis	1

Abbreviations: Tuberculosis-IRIS, Tuberculosis-immune reconstitution inflammatory syndrome; CLIPPERS, chronic lymphocytic inflammation with pontine perivascular enhancement responsive to steroids; MOG antibody-associated disease, Myelin oligodendrocyte glycoprotein antibody-associated disease

Supplementary table 6: Independent set of PFREL cases used for the algorithm validation.

Patient	Diagnosis	Sources
1	Subacute hemorrhage	Cliniques universitaires Saint-Luc
2	Metastases	Cliniques universitaires Saint-Luc
3	Pilocytic astrocytoma	Cliniques universitaires Saint-Luc
4	Pilocytic astrocytoma	Cliniques universitaires Saint-Luc
5	Hemangioblastoma	Cliniques universitaires Saint-Luc
6	Metastasis	Bose A, Prasad U, Kumar A, Kumari M, Suman SK, Sinha DK. Characterizing Various Posterior Fossa Tumors in Children and Adults With Diffusion-Weighted Imaging and Spectroscopy. <i>Cureus</i> . 2023 May 17;15(5):e39144. doi: 10.7759/cureus.39144. PMID: 37378152; PMCID: PMC10292159. Figure 6E
7	Abscess	Kumar, I., Shekhar, S., Yadav, T. <i>et al.</i> The many faces of intracranial tuberculosis: atypical presentations on MRI—a descriptive observational cohort study. <i>Egypt J Radiol Nucl Med</i> 54 , 116 (2023). https://doi.org/10.1186/s43055-023-01061-6 . Figure 4
8	Metastases	https://epos.myesr.org/posterimage/esr/ecr2015/129414/mediagallery/620694
9	Metastases	Bedre G, Gupta T, Rajasekharan P, Munshi A, Jalali R. Cerebellar, pancreatic, and paraspinal metastases in soft tissue sarcomas: unusual sites or changing patterns? <i>JOP</i> . 2007 Jul 9;8(4):444-9. PMID: 17625297.
10	Abscess	Renard, D., Castelnovo, G., Le Floch, A. <i>et al.</i> Pseudotumoral brain lesions: MRI review. <i>Acta Neurol Belg</i> 117 , 17–26 (2017). https://doi.org/10.1007/s13760-016-0725 . Figure 4
11	Abscess	Rafay, Muhammad & Sheikh, Muhammad & Aslam, Ejaz. (2018). Nocardia Brain Abscess in Immunocompetents. 10.31021/ijsp.20181108. Figure 1
12	Metastasis	Sharma SR, Maslin D, Ah-See SY, Todd P. Multiple cutaneous metastases as the first sign of metastatic carcinoma of unknown primary. <i>BMJ Case Rep</i> . 2018 Mar 9;2018:bcr2017223970. doi: 10.1136/bcr-2017-223970. PMID: 29523619; PMCID: PMC5847975.
13	Metastasis	Hôpital Erasme
14	Metastasis	Hôpital Erasme
15	Metastasis	Hôpital Erasme
16	Tuberculoma	Hôpital Erasme

Abbreviations: PFREL, posterior fossa ring enhancing lesion, Cliniques universitaires Saint-Luc, Cliniques universitaires Saint-Luc, Brussels, BE ; Hôpital Erasme, Hôpital Erasme - Hôpital Universitaire de Bruxelles, Brussels, BE